Advanced Drug Delivery Reviews 107 (2016) 136–152

Contents lists available at ScienceDirect

Advanced Drug Delivery Reviews

journal homepage: www.elsevier.com/locate/addr

Recent advances in degradable lactide-based shape-memory polymers☆

Maria Balk, Marc Behl, Christian Wischke, Jörg Zotzmann, Andreas Lendlein *

Institute of Biomaterial Science and Berlin Brandenburg Center for Regenerative Therapies (BCRT), Helmholtz-Zentrum Geesthacht, Kantstr. 55, 14513 Teltow, Germany

ARTICLE INFO

Article history:
Received 4 March 2016
Received in revised form 4 May 2016
Accepted 11 May 2016
Available online 1 June 2016

Keywords:
Shape-memory effect
Biodegradable
Polymer networks
Stimuli-sensitive
Lactide

ABSTRACT

Biodegradable polymers are versatile polymeric materials that have a high potential in biomedical applications avoiding subsequent surgeries to remove, for example, an implanted device. In the past decade, significant advances have been achieved with poly(lactide acid) (PLA)-based materials, as they can be equipped with an additional functionality, that is, a shape-memory effect (SME). Shape-memory polymers (SMPs) can switch their shape in a predefined manner upon application of a specific external stimulus. Accordingly, SMPs have a high potential for applications ranging from electronic engineering, textiles, aerospace, and energy to biomedical and drug delivery fields based on the perspectives of new capabilities arising with such materials in biomedicine. This study summarizes the progress in SMPs with a particular focus on PLA, illustrates the design of suitable homo- and copolymer structures as well as the link between the (co)polymer structure and switching functionality, and describes recent advantages in the implementation of novel switching phenomena into SMP technology.

Contents

☆ This review is part of the *Advanced Drug Delivery Reviews* theme issue on "PLA biodegradable polymers".

* Corresponding author at: Institute of Biomaterial Science, Helmholtz-Zentrum Geesthacht, Kantstr. 55, 14513 Teltow, Germany.
E-mail address: andreas.lendlein@hzg.de (A. Lendlein).

http://dx.doi.org/10.1016/j.addr.2016.05.012
0169-409X/

1. Introduction

Therapeutic devices such as implants, scaffolds, and drug release systems demand materials with controllable and adjustable properties. Biodegradable polymeric biomaterials are preferred candidates for their unique physical, chemical, and mechanical properties, which can easily be varied by the material composition and polymer architecture, and their degradation rates can be adjusted as required for an efficient therapeutical treatment. In the last decade, synthetic biodegradable polymers, such as poly(lactide acid) (PLA), poly(ε-caprolactone) (PCL), and its copolymers or blends, approved by the US Food and Drug Administration (FDA), have been widely used in medical devices as well as for fast wound healing or tissue repair [1–6]. In particular, PLA polymer networks based on dilactides are promising candidates for such applications, as their material properties are highly dependent on the conformation of the stereo center (LL, DD, or LD) (Fig. 1) and glass transition temperatures (T_gs) are close to the physiological relevant range.

At present, engineering of multifunctional materials has become an exciting strategy to overcome the limitations of the devices used in the fields of medicine and pharmaceutics. This includes the opportunities that arise from introducing the capacity of shape switching into medically accepted materials, which can be realized with shape-memory polymers (SMPs). SMPs are actively moving polymers, which can be deformed from a permanent to temporary shape and are able to recover the original, permanent macroscopic shape on the application of suitable external stimuli, such as temperature, magnetic field, light, electricity, and pH (Fig. 2) [7–18]. As the combination of this functionality with the degradability of the material is of special interest in the medical field, SMPs based on PLA were intensively discussed as highly innovative materials for future applications. For example, the synthesis, characterization, and paclitaxel release studies of an SMP double-layer system, whose layers based on trimethylene carbonate (TMC), glycolide, and L-lactide, were reported to be suitable for medical devices designed for endovascular applications [19]. Furthermore, biodegradable electrospun fiber scaffolds based on D,L-dilactide (DLLA) and TMC monomers featuring a shape-memory effect (SME) and bone-forming ability were shown [20]. Finally, yet importantly, a series of three-dimensional (3D) biodegradable shape-memory polyurethane scaffolds has been synthesized and applied for intravascular aneurysm embolization [21].

This study presents a comprehensive review of the recent progress and important developments related to degradable lactide-based SMPs. A wide overview of the latest applications, relationships between the properties and structure and morphology of SMPs, their synthesis and functions, as well as the PLA degradation mechanism are presented.

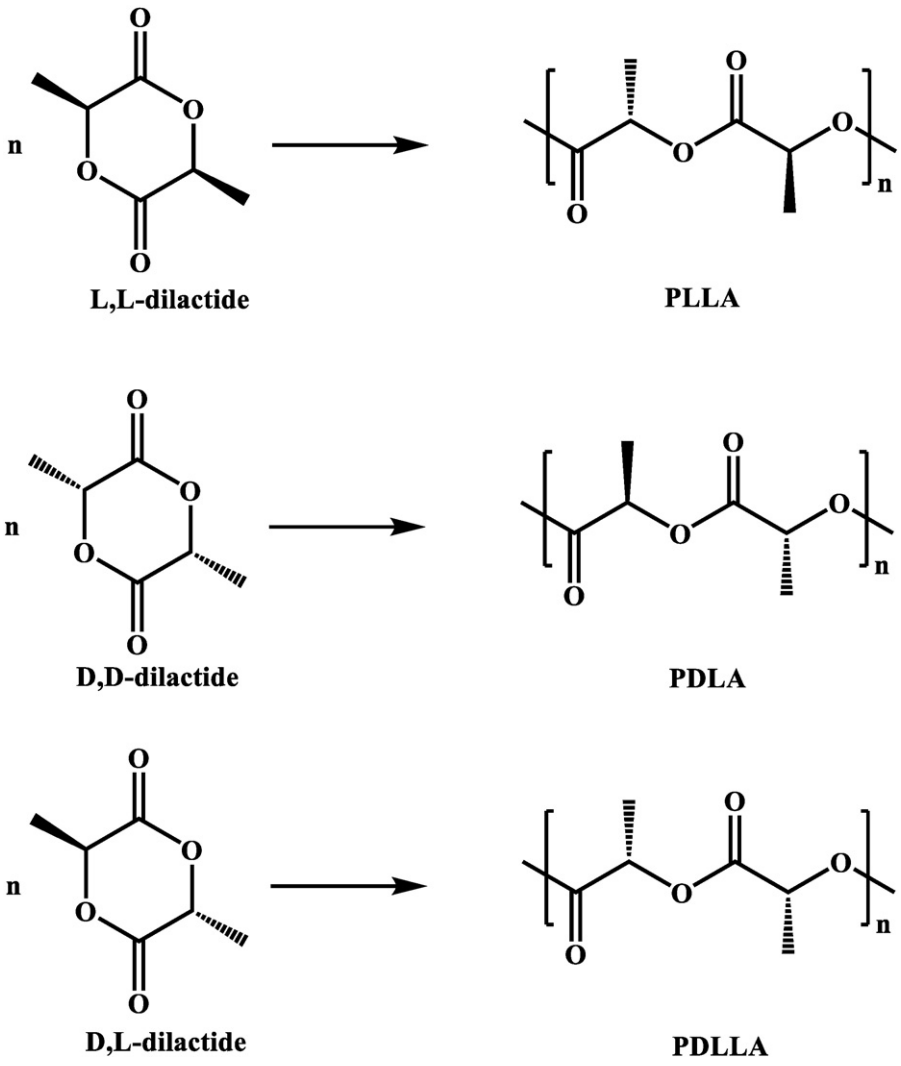

Fig. 1. Dilactides with different stereocenters and their polymers.

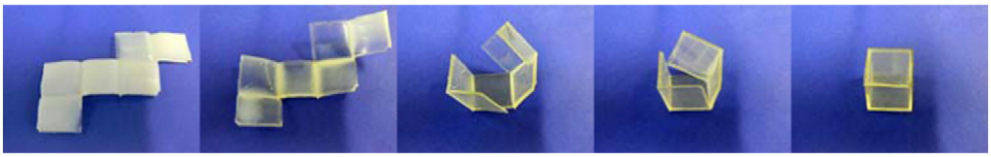

Fig. 2. Photo series showing the thermally induced SME of a cross-linked polymer. The SMP in its programmed temporary shape (left) is heated to 60 °C, from which it recovers within a time period of about 15 min to the permanent shape (right). Reproduced with permission from [9], © 2010 WILEY-VCH Verlag GmbH & Co. KGaA, Weinheim.

2. Application of biodegradable SMPs

Since the discovery of shape-memory alloys (SMA) [22] and the application of the SME in polymeric materials to be used in dental applications [23], the number of studies on SMPs has increase exponentially. Automotive, aerospace, robotic, and energy industries are examples of the research and application of smart materials [24–29].

This study progressed toward biomedical applications by the evaluation of temperature-sensitive SMPs based on polynorbornene in cardiac applications in 1990 [30]. Since then, comprehensive data have been collected on the biomedical applications of SMPs (Fig. 3). For instance, about 70% of patents recorded on SMPs in 2007 were focused on applications in biomedicine, for example, in hepatology, orthopedics, cardiology, and orthodontics [31]. This includes the use of SMPs in minimally invasive interactions or surgeries, such as smart sutures [32], removable stents [33–35], and aneurysm occlusion [36,37], as well as in drug delivery systems [38]. The limitations of short-term implantable materials in biomedicine, avoiding subsequent surgical procedures for implant extraction have been addressed by the development of degradable SMPs. In this sense, some current applications are described below.

2.1. In vivo tissue engineering

The provision of a three-dimensional material (scaffold) is one of the main components needed in most tissue engineering concepts. Porosity, pore size, pore connectivity, and chemical and mechanical properties determine the cell seeding, proliferation, and differentiation in the scaffold. It should be emphasized that 3D cell constructs cannot only be realized in the classical *in vitro* pre-seeding approach. Rather, an *in vivo* attraction of target cells appears as a promising concept. In this context, the development of cell/scaffold platforms using degradable SMPs as support materials has emerged. The material needs to attain a predefined shape to enable delivery to the application site by minimally invasive intervention. After implantation, the artificial extracellular matrix (scaffold) would be triggered to switch its shape and adapt the dimensions of the tissue defect. The scaffold should degrade according to a specific kinetics, allowing the ingrowth of tissue and the delivery of appropriate bioactive factors in the implant site. In this way, tissues might be restored in the future.

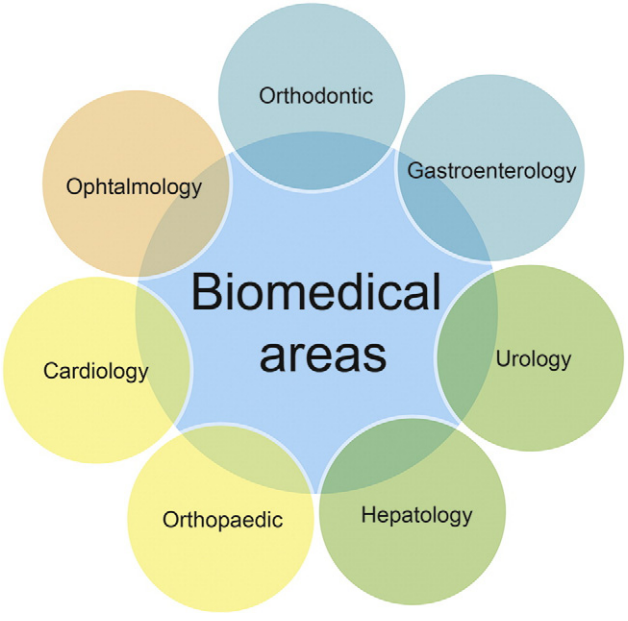

Fig. 3. Current and potential application fields of biodegradable SMPs in the biomedical area.

Recent examples include the development of multifunctional fibrous scaffolds based on poly(D,L-lactide) (PDLLA) and TMC, which combine the capability to mimic the bone tissue architecture with SME [20]. The *in vitro* results suggest that these fibrous scaffolds have good capability to promote osteoblast proliferation, maturation (osteogenic differentiation), and bone formation. Furthermore, scaffolds produced by salt-leaching technique based on terpolymers of LLA, glycolide, and TMC or on LLA, glycolide, and ε-CL exhibited the desired recovery of the permanent shape in a model defect of bone tissue, whereby the defect was filled within 12 min [39].

2.2. Drug delivery systems

Drug carrier systems from hydrophobic, slowly degrading polymers like PLA are typically designated for parenteral application and long-term release. This release can range from weeks up to several months depending, for example, upon drug properties and the length and quality of diffusion barriers provided by the implant or injectable carrier system. Also for SMPs, different sizes and designs of matrices can be realized, which include concepts for self-anchoring implant rods to avoid tissue migration [40] as well as shape-switchable microparticles [41,42]. Still, a number of frame conditions need to be considered for the selection of appropriate drug loading and processing techniques for SMP. In particular, as will later be discussed in more detail, polymer network structures are one precondition for realizing the SME. As shape switching, at least when recalling the SME for the first time, is often not quantitative for SMPs that only contain physical netpoints, the research on drug delivery from SMP has focused on covalently cross-linked polymer network with only a few exceptions [43].

In addition to the benefits of a typically quantitative switch to the designated shape for covalent SMP networks, the required cross-linking step may limit the available techniques in preparing, for example, drug-loaded SMP implant rods. So far, most studies have performed drug loading by either swelling a presynthesized polymer network in an organic drug solution or cross-linking network precursors in melt or solution in the presence of dispersed drugs, which, importantly, must not be modified under the selected reaction conditions. For a set of copolyester-based network materials, it was illustrated that loading by swelling may be associated with a higher initial drug release, because the drug was partially transported to the surface of the sample upon solvent evaporation [44]. Furthermore, it should be noted that, in some cases, amorphous networks from poly(lactide-*co*-glycolide) (PLGA) may behave beneficially compared to semicrystalline SMPs from other materials during drug loading by swelling, because PLGA networks showed no disturbance of the SME [45] and an increased accumulation of some types of drug during the swelling/loading step [46]. Regarding the application of relevant shapes of drug-loaded SMP implants, industrially feasible melt-based processing techniques such as coextrusion or

injection molding may be of interest. Reactive extrusion for in-line cross-linking [47] or high-energy irradiation at ambient conditions after processing to the designated shape [48] might be evaluated in the future.

For controlling drug release rates from SMPs, the use of copolymers with systematic variation of the comonomer content has been evaluated. It was shown for AB polymer networks comprising segments from oligo[(ε-caprolactone)-*co*-glycolide] and *n*-butyl acrylate that materials with increasing molar concentrations of the more hydrophilic glycolide units allow to increase release rates [49], as it is well established also for particles and implants from non-cross-linked PLGA based on an increased water uptake and drug diffusion coefficients in a plasticized matrix [50]. The drug release was also studied for SMP networks from diisocyanate-cross-linked four-arm star-shaped oligo[(*rac*-lactide)-*co*-glycolide] with a fixed glycolide content. Here, hydrophobic drugs showed a lag phase in their release profile, while a more hydrophilic model drug, ethacridine lactate, was released continuously for >4 months, indicating improved diffusivity in the hydrated SMP network [40]. A further study with similar material indicated that the precursor molecular weight, that is, increasing length of the telechels' arms and thus mesh sizes of the network, can be used to modify the release of aspirin [51]. Interestingly, also in studies conducted by the same coauthors of this study, matrix degradation interfered and significantly accelerated the drug release, which occurred after approximately 2 weeks or 2 months depending on the drug hydrophilicity/hydrophobicity [52]. This illustrates how drug-initiated mechanisms, such as osmotic water uptake, plasticization, or drug-catalyzed polymer degradation, can contribute to self-accelerated release patterns. Such profiles of initially slow and later more rapid release may be advantageous in some, but likely not in all clinical applications—at least if not externally controllable. Rather, a timely separation of the different functions of PLGA-based SMP networks without detrimental effects on each other may be appreciated: the SME for implant anchoring initially after placement was followed by a continuous drug release with low burst release, and finally implant removal by degradation [40].

Because the heat-induced SME is associated with a thermal transition, that is, substantial increase in polymer chain mobility and thus possibly enhanced drug diffusion, the initiation of the SME may allow initiating drug release. This concept was shown in principle to also enable a repetitive on-demand drug dosing together with a stepwise shape recovery, when applying high-intensity focused ultrasound (HIFU) for indirect heating [53,54]. Similar effects were also reported for pH-sensitive SMP materials, which showed hydration and thus enhanced drug diffusivity upon extreme pH changes [55]. Interesting applications may arise from further, ideally more application-specific container systems, where the SME should allow initiating the release of various types of bioactive molecules on demand [56].

3. Mechanism and characterization of the SME

SMPs are a class of materials that can be sensitive to changes in their environment by the change of the macroscopic shape [57,58]. While initially, scientific research was focused on thermally triggered movements in SMPs, current investigations have been expanded to other stimuli like UV light [18], near-infrared light [59], magnetic field [60], ultrasound [61], pH [62], and the presence of ions [63]. In addition to the most common SME, the one-way dual-shape effect (DSE), SMPs providing a triple-shape and multishape effect were reported, where two or more temporary shapes can be obtained [64,65]. Furthermore, the temperature at which the recovery process is initiated can be adjusted without changing the polymer composition by selecting an appropriate deformation temperature, as described for polymer networks possessing a temperature-memory effect (TME) [66,67]. Recently, the design of polymeric materials, which are capable of reversibly changing between two different shapes under load [68–70] and stress-free conditions [71–73] have been realized.

For the implementation of shape-memory properties, a polymer network architecture has to be created, which consists of either permanent netpoints generated by covalent bonds as in the case of chemically cross-linked polymer networks or strong interactions of polymer chains (e.g., hydrogen bonding and the formation of crystalline domains) forming a physically cross-linked polymer network (also called thermoplastic elastomer) to define the permanent shape. Permanent netpoints are interconnected by chain segments that contain molecular switches, which respond to external stimuli. These switches establish additional reversible cross-links within the polymer networks (denominated as temporary netpoints) to enable the fixation of a programmed temporary shape. SMPs can be designed by different molecular components, which are combined individually. For this reason, molecular architectures with permanent and temporary netpoints as well as chain segments providing sufficient elasticity present a modular system as shown in Fig. 4 [17].

In case of temperature sensitivity of molecular switches, a thermal transition associated to a switching temperature (T_{sw}) can be a T_g, liquid crystalline phase transition, or melting temperature (T_m). Shape fixation during programming is realized for such materials by vitrification or crystallization of the domains associated to the switching segment. Here, the main challenge is to freeze the elastic recovery, which can be achieved by reducing the mobility of polymer chains, for example, by lowering the bulk materials' temperature below a thermal fixation temperature of the SMP. Therefore, the stabilization of the temporary shape by a temporary fixation of the chain segments' conformation in the deformed state is the key requirement of SMPs. Such a reversible fixation can be achieved by solidification of the switching domains or the formation of additional chemical cross-links, which can be formed and cleaved on demand. Upon application of heat stimulus, these reversible cross-links are released allowing the permanent shape to recover. The stimulus-triggered recovery of the permanent shape is driven by entropic elasticity of the polymer network.

Fig. 5 shows the molecular mechanism of the thermally induced SME of covalently cross-linked SMPs. During a shape-memory experiment, the programming process comprises the elastic deformation of the SMPs from its permanent shape (B) above the T_{trans} of the switching segment. The fixation is achieved under either constant-stress or constant-strain conditions by establishing reversible cross-links when the temperature is decreased below this T_{trans}, which reduces the entropy of the polymer network. The temporary shape (A) is obtained when the external stress is released. The shape recovery process comprises the stress-free heating above T_{trans}. Here, the polymer chains return to the entropically favored random coil conformation as soon as they adapt to the rubber-elastic state. In the recovery process, the reversible cross-links are removed as a result of the application of an external stimulus, and the permanent shape (B) is recovered.

The quantification of the SME on the macroscopic level is typically based on the more relevant features, that is, the ability to fix deformation as a temporary shape during programming and recover the permanent shape. Commonly used variables are the percentage of strain fixation (strain fixity ratio R_f) and the extent of strain recovery (strain recovery ratio R_r) as determined in cyclic, thermomechanical tensile tests. These properties depend on parameters of the programming such as thermal conditions, kinetics, and type of deformation (elongation, bending, or compression).

Cyclic, thermomechanical tensile tests for quantification of the SME consist of two repetitive modules. The first module is the programming procedure, where the temporary shape is created and fixed. The second module consists of the recovery step, in which the permanent shape is recovered. The programming procedure can be performed stress- or strain-controlled while the recovery module can be carried out under stress-free or constant-strain conditions [57,74]. Thermomechanical parameters that affect the shape-memory properties are the applied

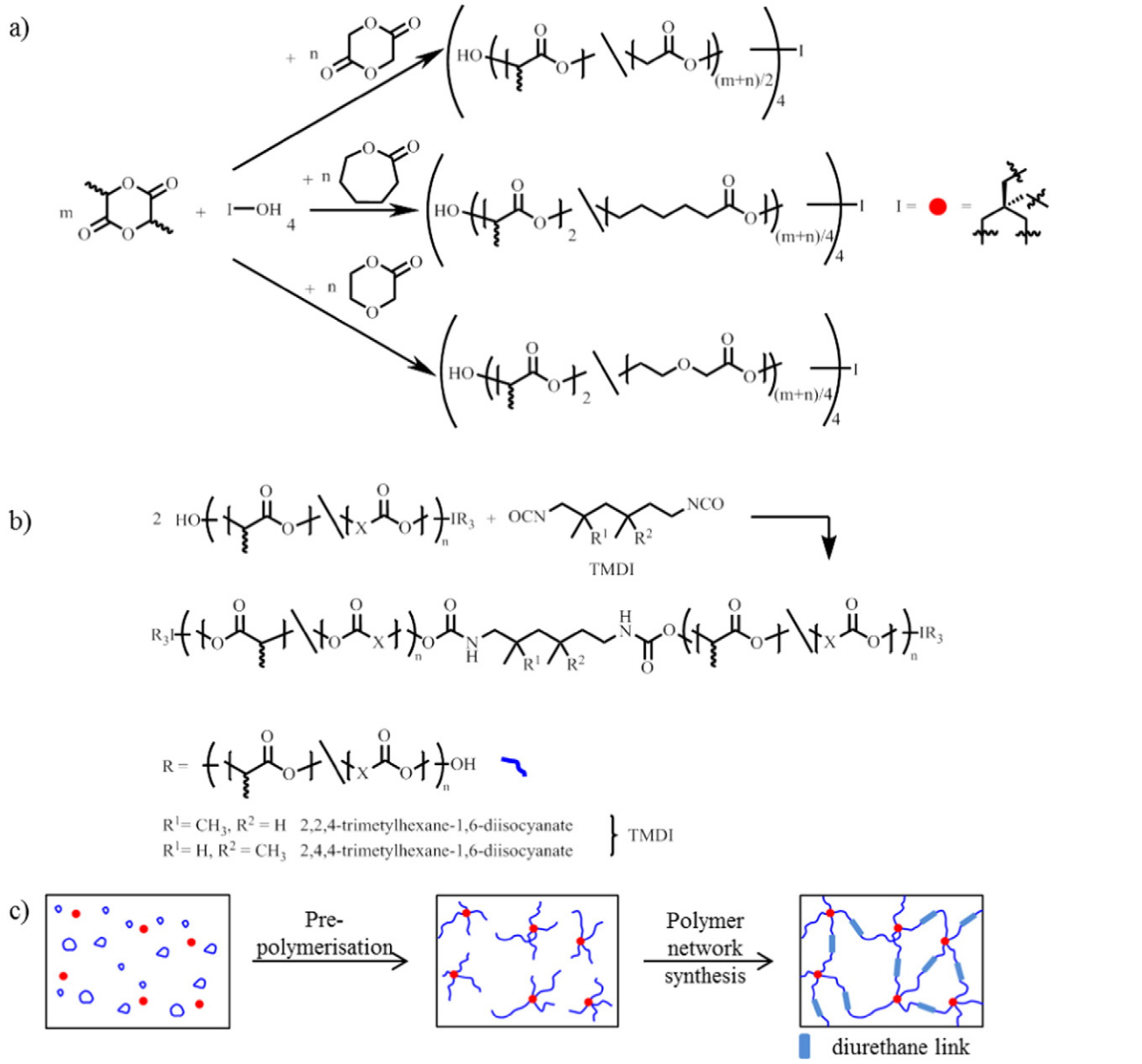

Fig. 4. Synthesis route of PLA-based SMPs with adjustable degradation rates and thermal properties as example for a modular buildup of SMPs. (a) Synthesis of copolymers by ring-opening polymerization initiated by a four-arm diol. Thermal properties and degradation rates are tailorable by the type and ratio of monomers as well as the type of initiator used for ROP. (b) Synthesis of polymer network structure with diisocyanate. (c) Scheme of the synthesis route and the obtained network architecture. Reproduced with permission from [17], © 2013 WILEY-VCH Verlag GmbH & Co. KGaA, Weinheim

strain, strain rate, cooling and heating rates, as well as the applied temperatures for deformation (T_{prog}), fixation of temporary shape (T_{low}), and recovery of the permanent shape (T_{high}).

The most commonly applied thermomechanical tensile test comprises a stress-controlled programming procedure performed with three programming steps as well as a recovery step under stress-free conditions (Fig. 6). In the programming step (I), the sample is heated to T_{prog} and stretched to a certain elongation ε_{prog} with a defined strain rate. During the programming step (II), the sample is cooled to T_{low} with a specific cooling rate, while the stress is kept constant at the maximum value, which was reached during the deformation of step (I). The elongation at T_{low} under load is characterized by ε_l. The sample is then unloaded in the programming step (III) by setting the stress to 0 MPa, which results in the temporary shape being represented by the elongation ε_u. After each change of the thermal or mechanical conditions, an equilibration time of a defined length is applied before the next step.

The shape fixity ratio R_f describes the ability to fix the mechanical deformation applied during the programming process in the temporary shape. It is given by the ratio of the deformation strain in the stress-free state after unloading of the tensile stress to the deformation strain before unloading. However, the recovery is rarely 100% so that except for the first cycle, the remaining strain after recovery (ε_p) from the previous cycle has to be subtracted. Eq. (1) applies for a programming procedure under stress control, where N denotes the number of cycles.

The programming can be performed in strain-controlled conditions by keeping the elongation constant during cooling and unloading at T_{low}. The parameter R_f is then determined by applying Eq. (2), where ε_l can be replaced by ε_{prog}.

After the programming procedure, the most common recovery experiment performed in the recovery module involves heating from T_{low} to T_{high} with a constant heating rate under stress-free conditions. After reaching T_{high} and allowing a certain equilibration time, the

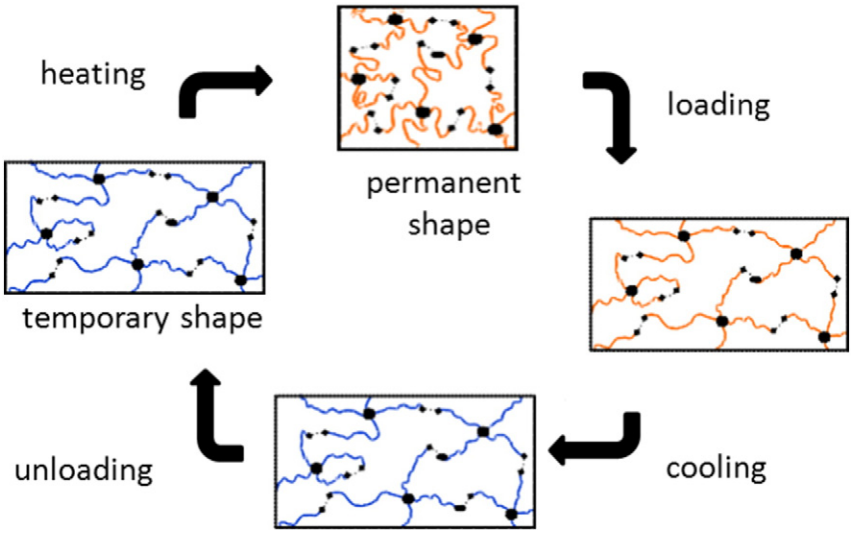

Fig. 5. Molecular mechanism of the thermally induced SME of amorphous cross-linked shape-memory polymers based on four-arm star-shaped precursors with short links connecting the ends of two arms; red lines represent the polymer chains of the switching segment at $T > T_g$ and blue lines at $T < T_g$, large black circles show the netpoints, and two connected small black circles represent the link. Adapted from [137] with permission, 2005 Wiley-VCH Verlag GmbH & Co. KGaA, Weinheim.

permanent shape is recovered being characterized by the elongation ε_p. The shape recovery ratio R_r quantifies the extent of shape recovery by relating the elongation after recovery with the elongation after programming according to Eq. (3) for the stress-free recovery. Furthermore, for the strain-controlled recovery, where the strain is kept constant and the stress is monitored during heating followed by an unloading step at T_{high} leading to ε_p:

$$R_f(N) = \frac{\varepsilon_u(N) - \varepsilon_p(N-1)}{\varepsilon_1(N) - \varepsilon_p(N-1)} \quad (1)$$

$$R_f(N) = \frac{\varepsilon_u(N) - \varepsilon_p(N-1)}{\varepsilon_{prog}(N) - \varepsilon_p(N-1)} \quad (2)$$

$$R_r(N) = \frac{\varepsilon_u(N) - \varepsilon_p(N)}{\varepsilon_u(N) - \varepsilon_p(N-1)} \quad (3)$$

The parameter T_{sw} is determined at the inflection point of strain–temperature curve $\varepsilon(T)$ from the recovery step, where the recovery rate is maximal (first derivation of the $\varepsilon(T)$ function reaches a minimum). As an additional value for quantification of the recovery behavior, the recovery temperature interval ΔT_{rec} is defined as the difference between the temperature at which the recovery starts and the temperature at which the recovery is completed. Because it is often difficult to determine the exact start and end of the shape recovery, the range-limiting temperatures are defined as temperatures at which a certain extent of the elongation is recovered; the frequently applied range is ΔT_{rec} between 10% and 90% recovery. Values of the discussed shape-memory characteristics are typically average values over several cycles, whereas the first cycle is usually discarded. Values from the first cycle often differ significantly from the values of the other cycles due to the thermomechanical history stored in the sample, which will affect only the first cycle (e.g., segment chain orientation and relaxation effects) and removed afterward.

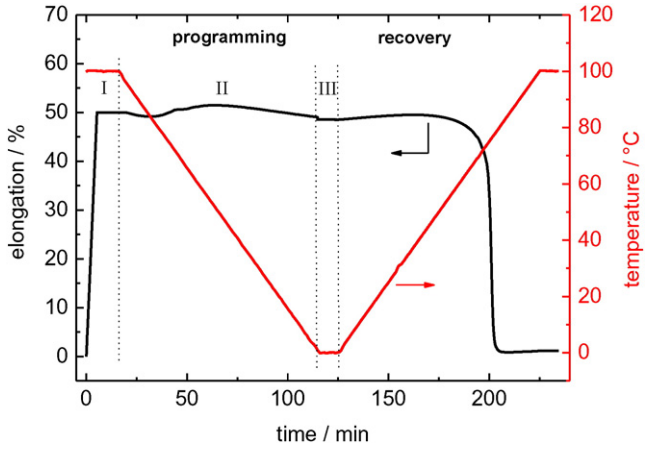

Fig. 6. One cycle of a thermomechanical tensile test; dependence of elongation and temperature during stress-controlled programming and stress-free recovery on time.

3.1. Dual-shape effect

The DSE is the most simple and common SME and a classic definition of SMPs, in which the polymer material can only recollect its original permanent shape achieved from a temporary shape (Fig. 7a). Here, the permanent shape is determined by permanent netpoints, whereby the temporary shape is fixed, when temporary netpoints are generated. In addition, several parameters affect the shape-memory performance of SMPs of DSE. For instance, the switching temperature of biodegradable shape-memory poly(*rac*-lactide) urethane networks could be systematically controlled by choice of the comonomer type and ratio such as ε-caprolactone (ε-CL), diglycolide, and *p*-dioxanone (Figs. 8 and 9) [75].

3.2. Triple-shape polymers

Smart triple-shape-memory polymers (TSPs) are able to store two metastable shapes (temporary shape A and temporary shape B). In the recovery process in response to certain external stimuli, the TSP switch back adapting these intermediated shapes until the permanent shape (shape C) is achieved. In general, physically and chemically cross-linked TSP networks, which contain a phase providing the netpoints and two independent switching phases associated with two different transitions, are capable of a triple-shape effect (Fig. 7b). For instance, SMPs with two crystalline switching phases combined with each other or a mixture of amorphous and crystalline domains were shown [76].

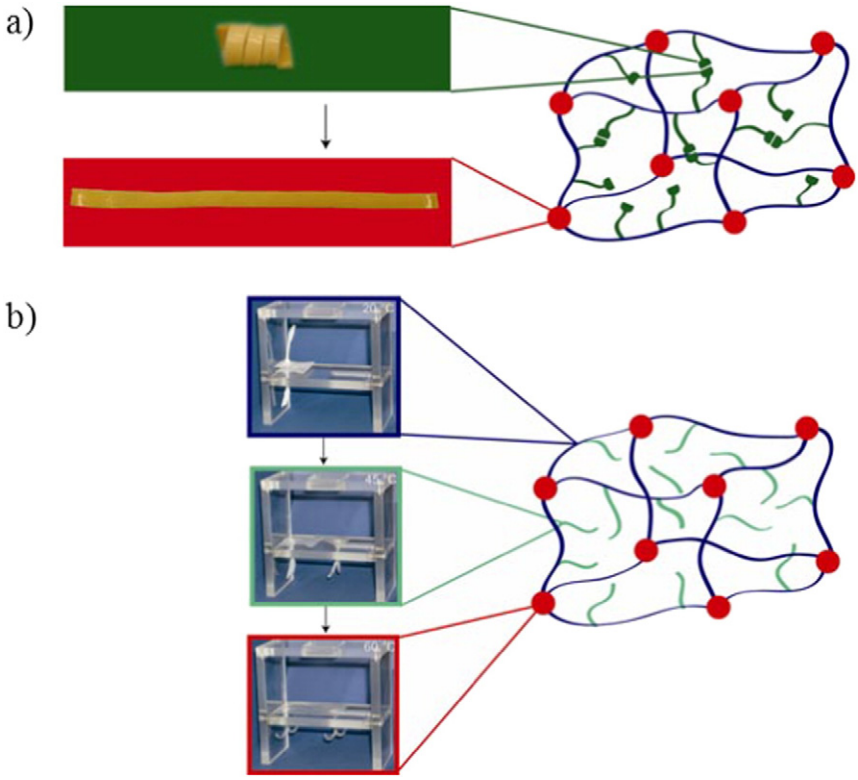

Fig. 7. Schematic illustration of a dual-shape (a) and triple-shape effect (b) on the macroscopic and molecular level. (a) The temporary shape is fixed by the formation of temporary netpoints (green) and after application of an external stimulus, the permanent shape is recovered, which is determined by permanent netpoints (red). (b) Polymer network exhibiting triple-shape properties. The temporary shapes are stabilized by two switching segments: the side chain (green) and the chain segment (blue). Reproduced with permission from [17], © 2013 WILEY-VCH Verlag GmbH & Co. KGaA, Weinheim, with figure parts from A. Lendlein, H. Jiang, O. Junger, R. Langer, Nature 2005, 434, 879 Copyright 2005, Nature Publishing Group and M. Behl, J. Zotzmann, A. Lendlein, Adv. Polym. Sci. 2010, 226, 1. Copyright, Springer-Verlag, Berlin, Heidelberg 2009; with permission of Springer.

3.3. Temperature-memory effect

A significant effect of the programming condition on the shape-memory behavior was reported to be independent of the recovery process. Polymeric materials providing a TME can recover the temperature applied in the programming procedure. This functionality can be realized with SMPs possessing a broad thermal transition area, whereby T_{sw} strongly correlates with the temperature, which was applied during deformation from the permanent shape to temporary shape. Therefore, the TME enables adjustment of the recovery temperature according to a specific application, whereby the synthesis of a new material can be avoided.

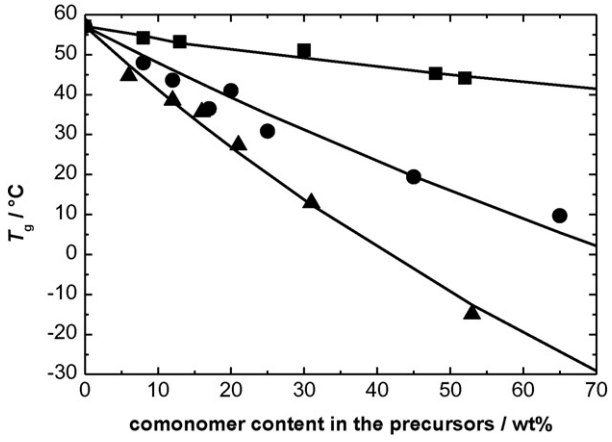

Fig. 8. T_gs and regression functions (lines) of polymer networks from star-shaped precursors based on poly(*rac*-lactide) depending on the comonomer content in the polyester precursors; incorporated comonomer: diglycolide (squares), ε-caprolactone (circles), *p*-dioxanone (triangles). Adapted from [75] with permission. Copyright 2009 American Chemical Society.

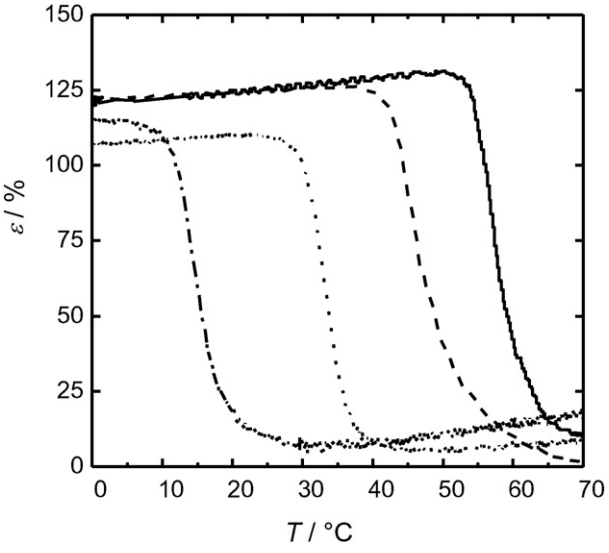

Fig. 9. Strain recovery process of copolyesterurethane networks under stress-free conditions in stress-controlled thermomechanical tests; networks were based on PLA precursors incorporating the following comonomers: solid line: diglycolide 17 wt%; dashed line: diglycolide 52 wt%; dotted line: ε-caprolactone 16 wt%, dot–dash line: ε-caprolactone 31 wt%. Adapted from [75] with permission. Copyright 2009 American Chemical Society.

3.4. Reversible bidirectional SME

SMPs having a broad melting temperature range can furthermore provide a reversible bidirectional SME (rbSME), whereby crystalline domains acting partially as actuator domains (ADs) and shifting-geometry determining domains (SGDs) [71–73]. By selecting the temperature of the programming process (T_{sep}), the crystalline domains from a broad thermal transition can be divided into ADs and SGDs. At this temperature, the degradable SMPs can be deformed and fixed by cooling to T_{low}. When the temperature is increased to T_{sep}, a melting-induced contraction can be obtained. A reversible movement is achieved by crystallization-induced elongation due to a decrease of temperature in the next step. This novel functionality has been realized recently with degradable SMPs based on oligo(ε-CL) segments having an average molecular weight between 2300 and 15,200 g·mol^{-1} [73]. The hydroxy end groups were functionalized with reactive methacrylate groups and chemically cross-linked copolymer networks were subsequently obtained by UV irradiation with *n*-butylacrylate as comonomer resulting in broad melting transitions. Here, 37 °C was selected as T_{sep}, resulting in reversible shape shifts in a temperature range relevant for biomedical applications (Fig. 10).

3.5. Influencing the shape-memory characteristics of SMPs

In general, the shape recovery ratio R_r reaches higher values in covalent SMP networks than those in thermoplastic SMP$_S$, which can be attributed to a better stability of the permanent shape especially at higher temperatures by using covalent cross-links. Creeping during programming is significantly reduced in covalent polymer networks, but bond breaking due to overstraining can result in lower R_r values.

Parameters for controlling the shape-memory behavior of covalently cross-linked polymer networks are the functionality of the cross-links, the molecular weight of the netpoint connecting polymer chains, and the nature of the switching segments. The functionality of cross-links and the molecular weight of the polymer chains control the cross-link density and thereby affect the mechanical properties, while the nature of the switching segments influences the characteristics of the SME, such as T_{sw}, fixation of the temporary shape, and recovery rate.

A strategy of lowering T_gs of amorphous switching segments is using the plasticizing effect of a solvent, which is typically water for biomaterials. T_g and correspondingly T_{sw} of PLGA copolymer networks having a glycolide comonomer content of approximately 20 wt% could be reduced by the uptake of water and the SME at body temperature could be enabled [77]. In this way, a solvent-induced indirect actuation of the SME was obtained in water at 37 °C. The SME of PLGA copolymer networks was triggered within several hours in water at the aforementioned temperature depending on the molecular weight of the star-shaped precursors, while no SME was observed after 1 day in water at 25 °C. Copolymer networks based on precursors having M_n of 3000 or 5000 g·mol^{-1} showed a complete recovery within 10 h of immersion time. However, for a polymer network from precursor with M_n = 10,000 g·mol^{-1}, R_r of only 40% after 1 day in water at 37 °C was obtained, which could be attributed to the lower cross-link density of the copolymer network.

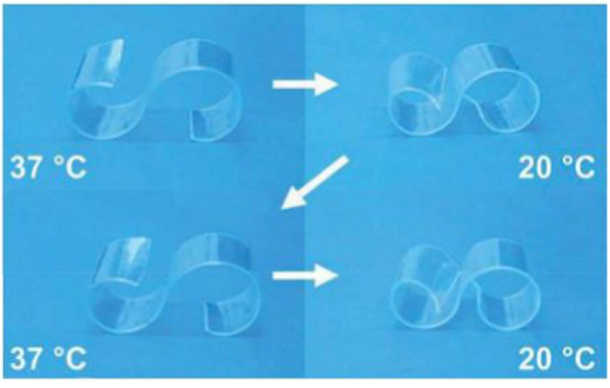

Fig. 10. Macroscopic view of the reversible bidirectional SME, which was realized with biodegradable SMPs. Reproduced with permission from [73]. © 2015 WILEY-VCH Verlag GmbH & Co. KGaA, Weinheim.

The shape-memory behavior of copolyesterurethane networks based on three different star-shaped copolyester precursors was investigated by programming under stress control, while the recovery was performed under stress-free conditions [75]. The values for R_r and R_f were always higher than 95%. T_{sw} correlates with T_g of the networks and could be controlled in a temperature range of −15 °C to 56 °C (Figs. 8 and 9). A vicinity of T_{sw} to body temperature is of special interest for biomedical applications, as found for lactide-based copolymer networks based on poly[(*rac*-lactide)-*co*-(ε-caprolactone)] (PLC) with 16 wt% ε-CL (T_{sw} = 34 °C) and poly[(*rac*-lactide)-*co*-(*p*-dioxanone)] (PLD) with 20 wt% *p*-dioxanone (T_{sw} = 38 °C).

4. SME in polylactide-based polymer networks

4.1. Degradable thermoplastic elastomers based on PLA homopolymers and composites

Physically cross-linked polymer networks comprising intermolecular interactions, for example, hydrogen bonding or crystalline domains, are denominated as thermoplastic elastomers. In contrast to chemically cross-linked polymer networks, they can be molten at high temperature or dissolved by suitable solvents. Thermoplastic polymers such as PLLA were reported as SMPs as this semicrystalline material achieves T_g in the range of 60 °C–70 °C (correlated with T_{sw}) and melting transition at about 150 °C–170 °C. The crystalline domains could act as permanent netpoints and can be used to stabilize the permanent shape [78]. Polymer films of the PLLA were obtained by compression molding above T_m or solvent casting. The shape-memory behavior of thermoplastic PLLA has been investigated as a function of deformation (bending angle), molecular weight, and number of shape-memory cycles [79]. It was reported that the permanent shape was almost completely recovered when a low deformation (8%) by bending was applied in the programming procedure. The efficiency of the recovery process decreased with increasing number of shape-memory cycles by about 10%, as some physical cross-links were destroyed until steady state was reached. Furthermore, R_r was not affected by the molecular weight (8000–25,000 g·mol^{-1}) of PLLA. Moreover, the efficiency of recovery was dependent on the deformation temperature with a decreasing recovery when the deformation temperature was increased [80]. The polymer chain orientation during programming was concentrated in the amorphous phase when the degree of deformation was low. In case of high deformation, the crystallinity increased, whereby R_r was drastically reduced. For this reason, the structure of PLLA and its change during the programming process affected the recovery behavior as also reported for PLLA multifilament yarns [81]. Here, a high degree of crystallinity and molecular orientation resulted in higher dynamic and static *E*-modulus, tensile strength, and lower elongation at break.

Furthermore, PDLLA as an amorphous polymer derived from D,L-dilactide was also presented, which exhibited the capability of a water-induced SME [82,83]. Here, the PDLLA was transferred into the temporary shape by an orientation-programming process resulting in stretched and oriented PDLLA (Fig. 11). The directed movement to the recovered shape was initiated at 37 °C in water, whereby a plasticizing effect similar to the descript PLGA copolymer networks [77] was achieved. The diffusion of water into the physically cross-linked thermoplastic elastomer cleaved intermolecular dipole–dipole and hydrogen bonding, which drastically reduced the T_g to about 12 °C. The temporary netpoints were released at R_r = 94% within 10 weeks.

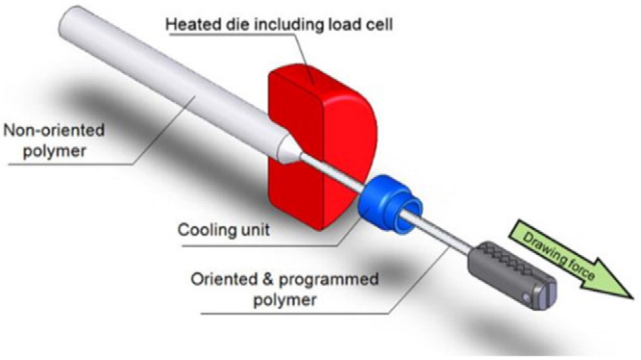

Fig. 11. Schematic illustration of the orientation-programming process of PDLLA. Taken from [82] © Springer Science + Business Media, LLC 2011. With permission of Springer.

A simple method to enhance the mechanical properties of PDLLA was obtained by solution blending with a stereocomplex (sc-PLA) of enantiomeric PLLA and poly(D,D-lactide) (PDLA) as reported recently (Fig. 12) [84]. This specific stereocomplex provides an important crystal modification resulting in higher melting transitions (220 °C–250 °C) as well as lower thermal and hydrolytic degradation rates [85–87]. The results showed the formation of complete stereocomplex crystallites, which could reinforce the PDLLA segments, increase the storage modulus when the sc-PLA content was increased, and enhance the shape-memory properties as the sc-PLA generates strong permanent netpoints. In addition, a delayed enzymatic hydrolytic degradation with proteinase K at 37 °C via surface erosion was found for PDLLA/sc-PLA blends.

In case of hard tissue application, the design of composite materials was reported to enhance mechanical properties. Hydroxyapatite (HA, $Ca_{10}(PO_4)_6(OH)_2$) as composite material provides excellent bioactivity, biocompatibility, as well as osteoconductivity [88–90] and was successfully introduced in SMPs based on PDLLA thermoplastic elastomers by solvent casting [91]. The composite-to-sample ratio was varied, whereby the sample thickness and composition affected the recovery time. An optimum shape recovery of >99% was obtained, which exceeded R_r for pure PDLLA samples, with samples exhibiting a PDLLA/HA ratio between 2 and 2.5. Here, hydrogen bonding between the C═O group of PDLLA and the surface P–OH of HA were detected by infrared spectroscopy (IR) and X-ray photoelectron spectroscopy (XPS) [92], which acted as a steady stationary phase and could therefore enhance the shape-memory property. A similar trend was noted when hybrid nanocomposites were designed via *in situ* grafting polymerization of HA and DLLA (Fig. 13) [93]. Here, it was found that the nanocomposites with varied HA content between 5 wt% and 25 wt% provided an improvement in recovery compared with pure PDLLA. In addition, materials having a covalent bond between HA and PDLLA enabled higher R_r values than composite blends (control material).

Another interesting candidate as inorganic filler presents β-tricalcium phosphate (TCP, 4β-$Ca_3(PO_4)_2$). Excellent shape-memory properties were reported for PDLLA/TCP composite materials. A systematic degradation study was conducted in phosphate-buffered saline (PBS) at 37 °C, and the interaction mechanism between PDLLA chains and the inorganic particle were analyzed [94]. For samples preincubated in PBS, R_r decreased within 56 days from 98%–96% to 67%–56%. This decrease was related to the cleavage of ester groups as monitored by gel permeation chromatography (GPC) measurements, which induced a decrease in T_g and the scission of entanglements acting as physical cross-links. In addition, as a result of degradation, a phase change of TCP was indicated by the formation of $Ca_2P_2O_7$, $CaHPO_4$, and HA, which affected the hydrogen bonding between PDLLA and the inorganic material, thereby reducing the recovery efficiency.

The formation of hydrogen bonds was furthermore detected for nanocomposites consisting of PDLLA and magnetite (Fe_3O_4). The interfacial interaction increased the tensile strength while the elongation at break (ε_b) was reduced. However, the presence of magnetic nanoparticles with a diameter of 20 nm enabled stimulus sensitivity to an alternating magnetic field and therefore an alternative approach was followed to recover the original shape [95].

In addition, SMP blends consisting of PLLA homopolymers and poly(methyl methacrylate) (PMMA) were reported to be capable of multi-shape transitions [96,97]. Blends were prepared by twin-screw extrusion. Thermal analysis of the obtained thermoplastic elastomers with a weight ratio of 1:1 showed a broad T_g between 60 °C and 100 °C. These physically linked polymer networks exhibited a DSE, as well as TSE, which was obtained by a two-step programming procedure at different temperatures. Furthermore, a TME was successfully obtained for these materials using the broad range of glass transition temperature.

The incorporation of glycolide as another biodegradable component into thermoplastic lactide-based SMPs is a possibility to reduce the T_g of PLLA toward the physiologically relevant range. For example, a fully degradable SMP was designed by solvent-casting of a mixture of PLLA and poly(glycolic acid) (PGA). This thermoplastic elastomer was processed

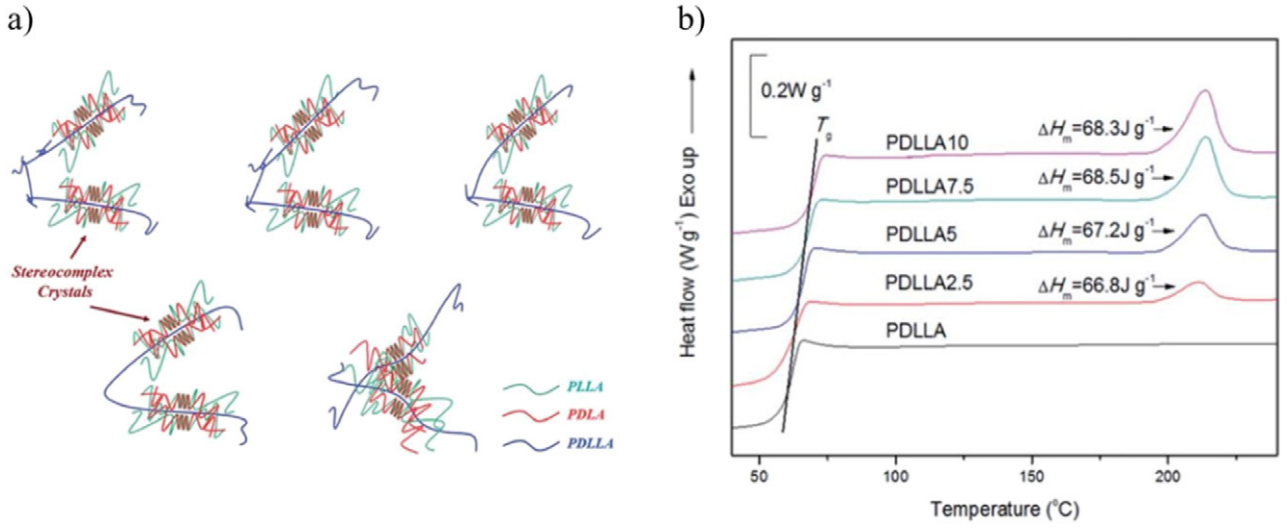

Fig. 12. (a) Potential structures of stereocomplex crystals in sc-PLA networks. (b) Thermal properties of sc-PLA networks PDLLA(*x*), where *x* represents the total content (in wt%) of PLLA and PDLA (ratio 1:1). Reproduced from [84] with permission of The Royal Society of Chemistry (http://dx.doi.org/10.1039/C5RA01624J).

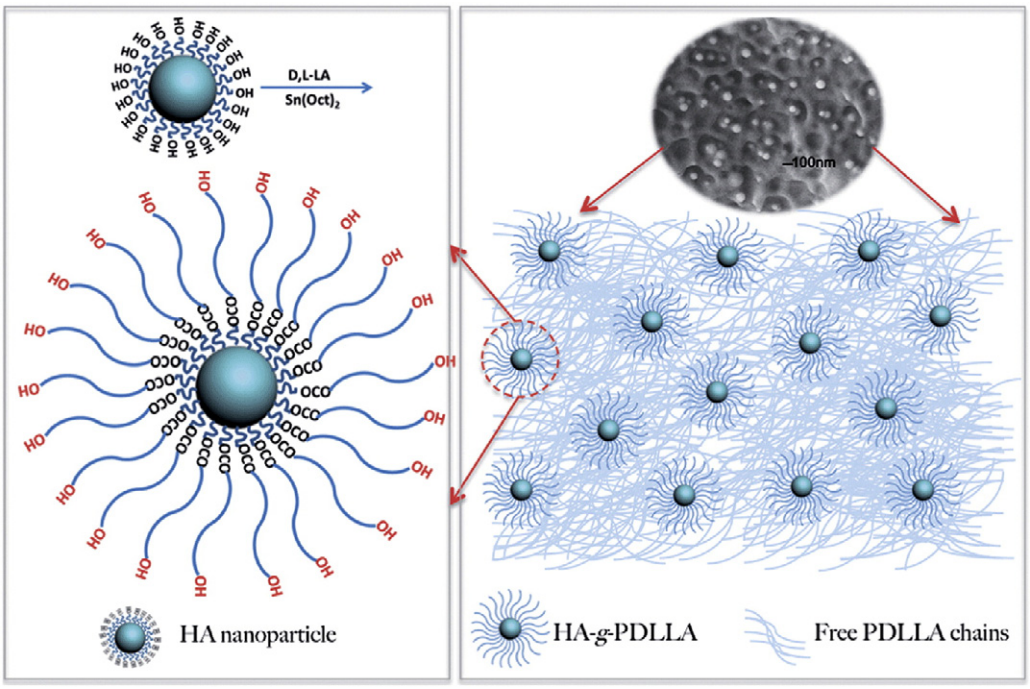

Fig. 13. Schematic illustration of hybrid nanocomposite formation with HA as initiator for ROP of DLLA. Reproduced from [93] with permission of The Royal Society of Chemistry (http://dx.doi.org/10.1039/C3TB21861A).

to a stent prototype, which exhibited self-expansion at body temperature [34].

4.2. Chemically cross-linked PLA homopolymers

Besides thermoplastic PLA homopolymers, chemically cross-linked PLA networks were studied, in which possible creep phenomena are retarded by covalent bonds. When the thermoreversible Diels–Alder reaction was used for the formation of covalent cross-links, recyclable SMP networks were obtained, which would easily be cleaved when the temperature is increased above the bond dissociation temperature of 160 °C [98–101]. Here, four- or six-arm PLLA was end group functionalized with furan moieties and cross-linked with a maleimide linker under heating conditions. The mechanical strength was increased when the linker consisted of flexible units such as hexamethylene dimaleimide or dodecamethylene dimaleimide.

Recently, PLLA networks have been investigated as degradable and electrically conductive materials with shape-memory properties to regulate cell activities [102]. Six-arm PLLA macromolecules were synthesized with inositol as initiator for ring-opening polymerization (ROP) of LLA. Here, the initiator acted as chemical netpoint as required for SMPs. An aniline trimer was incorporated with hexamethylenediisocyanate (HDI) to equip the SMP with electroactivity. The obtained mechanical properties were tunable in the range of GPa (37 °C) and the PLLA-based materials possessed high fixity and recovery ratios with a short recovery time when the temperature was increased. Furthermore, it was shown that the cell proliferation (mouse myoblast cell line) and osteogenic differentiation were significantly enhanced, which are important factors for bone tissue engineering.

4.3. Thermoplastic, elastomeric copolymer networks

SMPs based on PLA possessed shape-memory properties when the networks were heated above T_g ranging between 60 °C and 70 °C. In order to adjust the SME to body temperature as desired for the use in biomedical applications, various studies were performed on copolymer

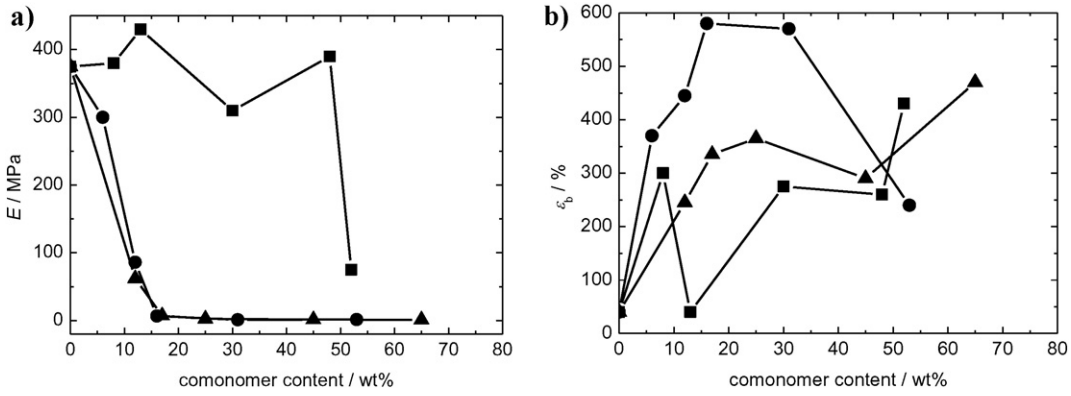

Fig. 14. Mechanical properties of networks from star-shaped copolymer precursors based on poly(*rac*-lactide) as functions of comonomer content in precursors; lines are guidelines for the eye: (a) Young's modulus; (b) strain at break; incorporated comonomers; (squares) diglycolide; (circles) ε-caprolactone; (triangles) *p*-dioxanone. Adapted from [75] with permission, copyright 2009 American Chemical Society.

networks, whereby the thermal and mechanical properties (Fig. 14), as well as shape-memory function and the degradation behavior can be modulated by the comonomer/copolymer content and type.

PLLA-*co*-PEG (poly(ethylene glycol)) copolymer-based polyester urethanes (PEUs) were synthesized by ROP of LLA with PEG-diol as initiator [103]. These triblock copolymers were subsequently linked in a polyaddition reaction using 4,4′-methylene diphenyl diisocyanate and 1,4-butandiol (as hard segment providing permanent netpoints) to obtain PEUs, in which PLLA-*co*-PEG was the soft segment (acting as switching domain) (Fig. 15). A broad range of T_gs between 0 °C and 57 °C was achieved by the variation of the PEG chain length (600–6000 $g \cdot mol^{-1}$) and soft-to-hard segment ratio. In addition, the elastic moduli were affected by the chain length of the soft segment and an almost complete recovery of the permanent shape was achieved when the hard segment content was >65%.

Another study showed the effect of stereocomplexation between PLLA and PDLA incorporated in triblock copolymers on microphase separation and mechanical and shape-memory properties [104,105]. The SMPs were synthesized by ROP of LLA and/or DLA with poly(ethylene-*co*-butylene) as initiator. An increased T_m from 160 °C to 220 °C was detected for enantiomeric blends because of the formation of PLLA–PDLA stereocomplex crystallites. The microphase-separated morphologies of PLLA–PDLLA-based blends showed spherical, cylindrical, and laminar structures (dependent on the PLLA content), whereby a less-ordered morphology was detected for stereocomplexes as evaluated by SAXS measurements.

During the past decades, much work was focused on the synthesis of poly[(L,L-dilactide)-*co*-(ε-caprolactone)] (PCLA) copolymers as PCL has been widely used in the medical field due to its degradability and biocompatibility [106]. Semicrystalline random PCLA copolymers were synthesized by ROP of LLA and ε-CL. While the PLLA crystals acted as physical cross-links (permanent netpoints), the amorphous fraction behaved as reversible switching phase [107–110]. Here, the T_g of PLLA was reduced to 14 °C–54 °C. Furthermore, the intrinsic viscosity of the networks was increased with increasing ε-CL content, resulting in enhanced shape-memory properties. Furthermore, the R_r decreased with deformation strain, because the PLLA crystals were deformed. The ε-CL content also significantly affected the tensile strength and ε_b, resulting in lower strength and higher ε_b with increasing wt% of ε-CL [111]. A higher degradation rate with a mass loss up to 35 wt% within 200 days was achieved with the SMP having the highest ε-CL content. Here, the cleavage of ester groups decreased R_r and the recovery stress.

Another strategy to design SMPs based on PLLA and PCL is to synthesize polyurethanes by ROP of LLA, which was initiated by PCL-diols to obtain a triblock copolymer, and subsequently by polyaddition of these triblock copolymers with HDI [112]. In these polyurethanes, the PCL formed crystalline domains, as PLLA and PCL were phase-segregated and thus T_{sw} correlated with T_m of PCL, which was close to body temperature. Excellent shape-memory properties in terms of R_f and R_r were observed for all tested elongations between 50% and 350%.

One of the most used synthetic biodegradable copolymers for applications as drug delivery system or in tissue engineering is PLGA [53,113,114]. For SMPs based on PLGA nanoparticles, a noncontact method was reported, whereby external heating can be avoided. Here, rather than magnetic nanoparticles, which can generate heat by the application of an alternating magnetic field, HIFU was used as stimulus for the shape recovery process (Fig. 16) [54]. Compared with magnetic actuators, the application of HIFU provides a safer and effective stimulus, as additional components (magnetic particles) are not required. Furthermore, it is used as a noninvasive surgical tool and the generated acoustic waves can interact with PLGA chains to increase the temperature. In addition, when the SMPs were loaded with proteins, the application of HIFU also induced an on-demand release.

Thermoplastic elastomers consisting of PLLA, PCL, and PGA were additionally investigated as SMPs, as PLLA and PCL could act as hard and soft segments, respectively, whereby the glycolic acid units would accelerate the degradation of the material. For example, multiblock copolymers were synthesized by polyaddition of PLLA-diols with poly[glycolide-*co*-(ε-caprolactone)]-diols [115]. The mechanical properties could be adjusted by modifying the PLLA content and chain length. The determination of degradation rate showed the degradability of these SMPs as a function of glycolide content, which was obtained between 1 and 2 months.

Recently, blends consisting of PLGA and PCLA have been investigated as SMPs for blood-contacting applications, as a reduced fibrinogen adsorption and platelet adhesion compared with PCLA, PLGA, or collagen were shown [2]. Furthermore, cell proliferation and alignment indicated the potential use as cellular matrix for stem cell differentiation. In addition, when PCLA was reinforced with PGA by *in situ* fibrillation, a strong interaction of PGA with the copolymer matrix was obtained, whereby the recovery ability was increased compared with PCLA [116].

One possibility to enhance mechanical and thermal properties of thermoplastic elastomers based on copolymers, for example, PCL–PLLA block copolymers, was the reinforcement by the design of composite materials [117]. In this case, the cellulose nanocrystals were used as bionanocomposites. As a result, the thermal degradation of the PCL block was shifted to higher temperatures, while degradation of PLLA remained constant. A decrease of thermal stability was observed when

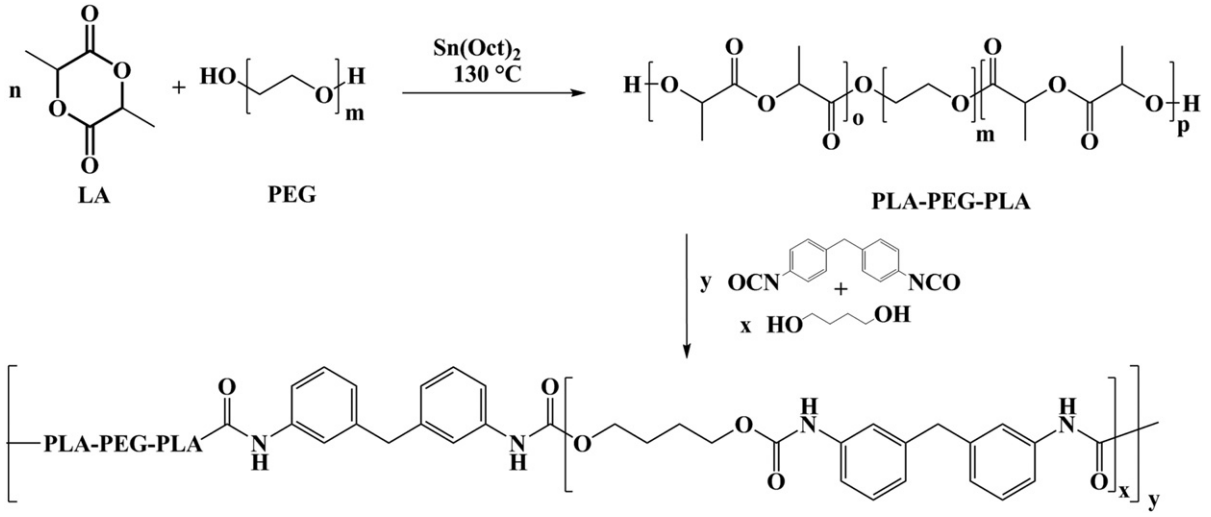

Fig. 15. Synthesis route of PLLA-co-PEG polyester urethanes with PEG as initiator. Adapted from [103] with permission. Copyright © 2011 John Wiley & Sons, Ltd.

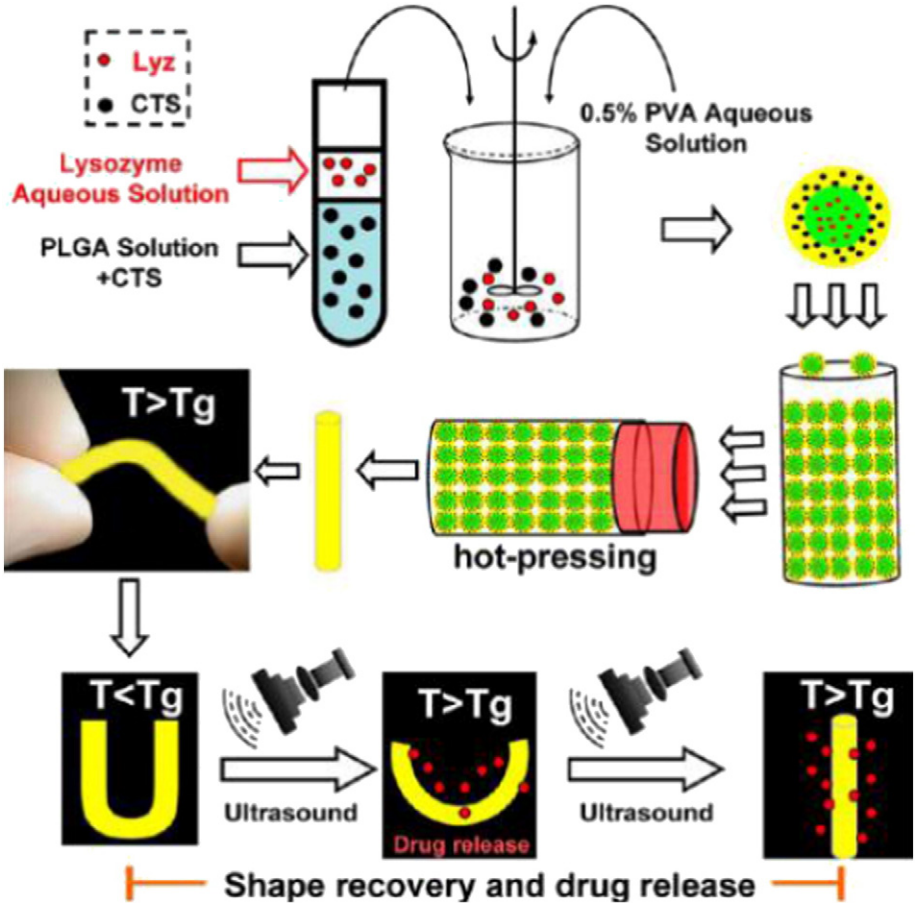

Fig. 16. Schematic illustration of the preparation of PLGA nanoparticles and thermoplastic elastomers by hot-pressing, shape recovery, and on-demand drug release after application of high-intensity focused ultrasound. Reprinted with permission from [54]. Copyright 2013 American Chemical Society.

HA was used as composite material [118]. The HA strongly affected the crystallinity as well as T_m of the PCL blocks, as HA preferentially interacted with a PCL-rich phase. In a low content, HA acted as plasticizer, whereas a reinforcement was obtained with a higher HA content (>3 wt%).

Reinforcing with a strong filler like inorganic composite materials was also reported for random PCLA. Here, for example, $CaCO_3$ whiskers (rod-shaped single-crystal fiber) were mentioned, as $CaCO_3$ was safe to use in clinical settings [119]. The obtained composite materials exhibited uniform distribution of the inorganic component in the polymer matrix, a slight increase in T_g, excellent elastomeric behavior with high ε_b (480%–600%), and increased storage moduli. When the $CaCO_3$ content was increased, R_f increased from 75% to 99%, whereas R_r decreased from 86% to 65%. In addition, multiwalled carbon nanotubes (MWCNTs) were investigated as potential filler material to obtain a reinforcing effect. The incorporation of MWCNTs resulted in a higher degree of crystallinity in PCLA copolymers, whereby R_f and R_r were slightly increased [120].

4.4. Chemically cross-linked copolymer networks

The presented PLA copolymer networks are based on physical cross-links, whereby they could exhibit poor shape stability due to irreversible viscous flow. As covalently cross-linked systems should not have these drawbacks, they are suitable for long storage before use due to their high dimensional form stability. Also for cross-linked copolymers, the thermal, mechanical, and shape-memory properties can be controlled by the incorporation of different comonomers or copolymers [121,122]. One possibility was the synthesis of chemically cross-linked copolymer networks by thermal cross-linking of PLLA and PEG blends with diisocyanates [123]. In comparison with non-cross-linked blends, cross-linked SMPs exhibited enhanced mechanical properties and higher R_f and R_r values. Furthermore, the photo-cross-linking of end group-methacrylated copolymers, for example, poly(DLLA-*co*-TMC), has been reported recently [124]. In these systems, a glass transition temperature between −13 °C and 51 °C was obtained as a function of the TMC content, as poly(TMC) is amorphous with the T_g of about −15 °C. The *E*-moduli were significantly affected by the composition and adjustable between 5.3 Pa and 2450 Pa; ε_b of up to 800% were achieved. These SMPs were molded into a spiral shape (for vascular stenting) and complex anchor structures (as an occluder in closing soft defects), as well as in porous scaffolds (as volume-filling material) to show their high potential for biomedical applications. Furthermore, an annulus fibrosus closure device was prepared with a DLLA to TMC molar ratio of 60:40, which could be inserted minimally invasively in the disk of a cadaveric canine spine [125].

In addition to the presented SME induced by heat, water, magnetic field, and HIFU, recently, a light-induced SME has been established in PEUs consisting of PLLA-diols as hard segment, which were connected to PCL-diols as soft segment by means of a diisocyanate linker [126]. Here, the introduction of the photoresponsive *N,N*-bis(2-hydroxyethyl) cinnamamide enabled the cross-linking reaction via [2 + 2] cycloaddition reaction when exposed to >260 nm UV light (Fig. 17). As these temporary cross-links can be reversibly cleaved upon irradiation with UV light >260 nm, the presented system exhibited shape-memory properties at room temperature and the properties of this functionality were affected by the content of photoresponsive groups.

Furthermore, the copolymerization of lactides with glycolid units was reported. Here, a series of degradable poly[(L,L-dilactide)-*co*-

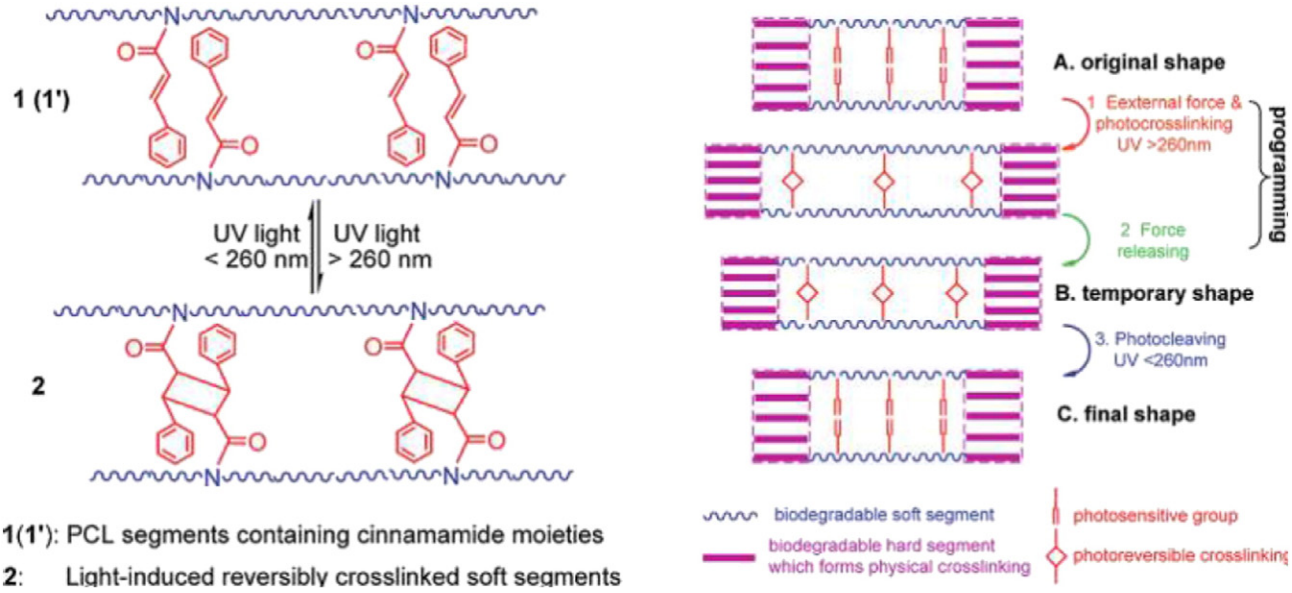

Fig. 17. Schematic illustration of the light-induced SME in PLLA/PCL polymer networks, in which the photoresponsive cinnamamide units acted as temporary netpoints. Reprinted with permission from [126]. Copyright 2011 American Chemical Society.

glycolid] copolymer networks were synthesized with a random sequence structure, which was obtained by transesterification using dibutyltin oxide as catalyst [127,128]. The cross-linking reaction was performed by UV irradiation of end group-methacrylated copolymers. The random structure resulted in completely amorphous copolymer networks. While *E*-moduli were affected by the cross-linking density, T_g was not affected and was almost constant at 55 °C. Excellent shape-memory properties with R_f and R_r > 99% were achieved when a fixity temperature (T_{low}) just below T_g was selected, which was related to a low stress increase during fixation minimizing irreversible bond breakage. In order to obtain a high elasticity even below T_g, a second amorphous phase (ethyl acrylate, butyl acrylate, or hexyl acrylate) with a lower glass transition was incorporated [129]. Here, phase separation was achieved with hexyl acrylate, whereby a clearly enhance elasticity was detected. Because of the presence of two separated T_gs, these two-phase systems have the potential to exhibit triple-shape functionality.

5. Degradation mechanism of biodegradable SMP networks

The use of temporary SMP networks for biomedical devices requires a profound investigation of their biocompatibility and biodegradability. Biodegradable SMPs are intended to operate for a specific time period and are then supposed, depending on the material type, to be eliminated from the human body through a controlled mechanism. In this way, the risk of medical problems related to the long-term exposure of foreign materials should be reduced and, on the contrary, the need for other surgeries for implant removal is avoided, which are some of the advantages of biodegradable SMPs upon the addition of permanent polymer materials.

In addition, in the case of application of biodegradable SMPs for drug delivery, the physical and chemical properties of SMPs determine the type of degradation mechanisms and therefore the drug release profiles. Two types of degradation mechanisms have to be considered: degradation by chemical hydrolysis and enzymatic degradation. Details of the chemical and enzymatic degradation mechanisms of SMPs are described below.

5.1. Degradation by chemical hydrolysis

Biodegradation of polymers is mainly caused by hydrolytic bond cleavage. In addition to the hydrolysis rate, the rate of degradation is determined by diffusion processes; mainly, the diffusion of water into and small degradation products out of the polymer matrix. In general, two mechanisms of biodegradation can be differentiated depending upon the ratio of the rate of hydrolysis to diffusion [130]. Surface degradation shows linear degradation characteristics, directed from the surface to the center of the polymeric implant. Here, the diffusion is slow and confines the degradation to the area near the surface, while the hydrolysis rate is high (Fig. 18a). The implant is permanently reduced in size, but sustains its integrity and properties in parts distant from the surface. By contrast, bulk degradation is a nonlinear process. Diffusion is faster than hydrolysis, thereby allowing degradation to take place all over the polymer matrix. Within a material-specific induction time, mechanical properties deteriorate without size reduction of the polymer body during the generation of larger degradation products. After that time, the degradation products become small enough to diffuse out of the polymer matrix and the implant disintegrates with a fast mass loss. The effective degradation behavior often shows a mixture of characteristics from both models depending on diffusion rate, hydrophilicity, and homogeneity of the implant material. Amorphous polymer networks show a more homogenous degradation than crystallizable polymer networks, which is advantageous for application as implant materials.

Hydrolytic degradability of SMPs can be realized by the introduction of weak hydrolyzable bonds, which can be easily cleaved under physiological conditions [131]. Therefore, the class of (co)polyesters is mostly applied for such biomaterials. The ester bond can be cleaved hydrolytically, whereas the rate of hydrolyzation depends on the nature of the (co)monomers. However, another influencing factor is the steric accessibility of the ester bonds, as hydrolytic degradation is hindered by bulky substituents.

The sample mass after a degradation period t_d relative to the original sample mass $m(t_d) \times m_0^{-1}$ is used to show the mass loss due to the release of water-soluble products during degradation.

In case of PLA, the hydrolytic cleavage of ester groups is highly affected by the stereocenter. While a heterogeneous hydrolytic degradation with a higher rate in the internal material than the polymer surface was reported for amorphous PDLLA [132], semicrystalline PLLA possessed two stages of ester scission [133]: (1) the random hydrolytic cleavage of ester bonds in amorphous domains, resulting in an increasing crystallinity and (2) the degradation of the crystalline fraction from the edge toward the crystal center. On the contrary, stereocomplexes,

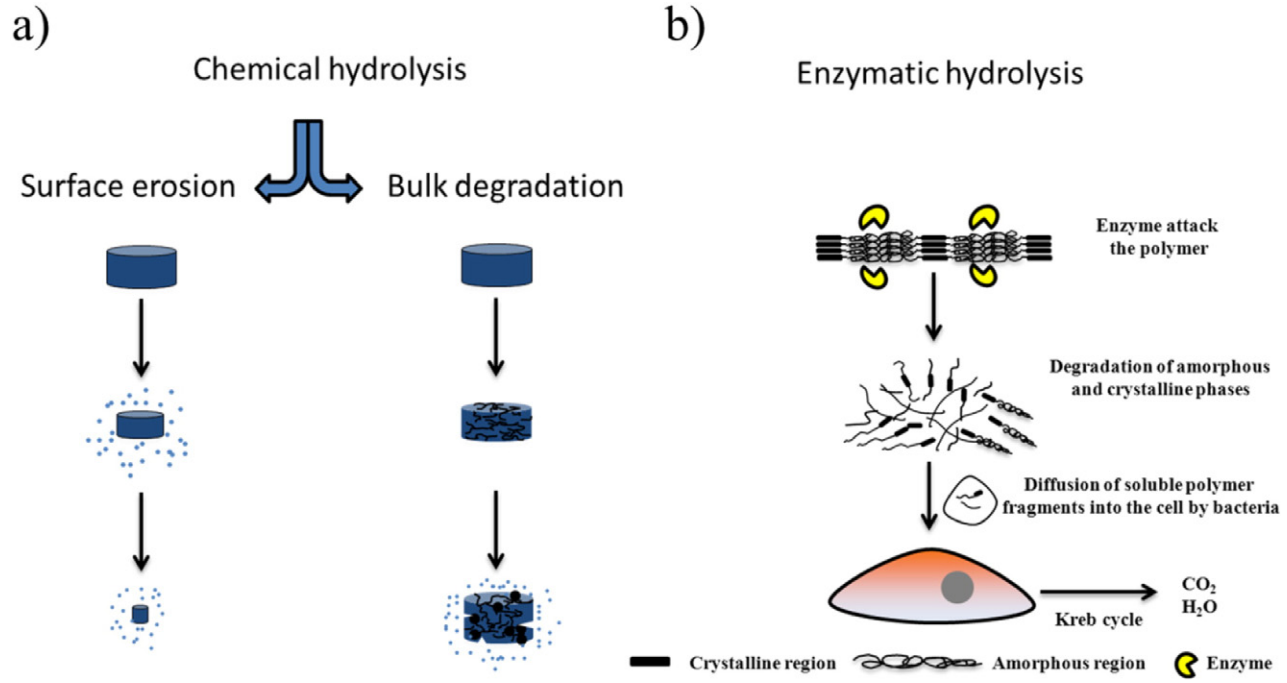

Fig. 18. Degradation mechanisms by chemical hydrolysis (a) and enzymatic hydrolysis (b).

which can be formed during degradation, possessed high resistance toward hydrolytic ester cleavage [134].

Hydrolytic degradation experiments carried out on copolyesterurethane networks based on star-shaped PLGA precursors showed three phases of degradation [135]. In the first phase, the mass was unchanged, which indicates bulk degradation. The second phase was characterized by accelerated mass loss and the third phase showed retarded mass loss (Fig. 19). In the first phase called induction period, water diffused into the polymer networks and started hydrolytic cleavage of copolyester segment chains. The diffusion of water is affected by the hydrophilicity of polymer networks and increased with increasing glycolide content of the copolyester network. During this period, the partly degraded chain segments were still connected to the network. In the second phase, hydrolysis generated degradation products being small enough to diffuse out of the polymer network and causing the mass loss.

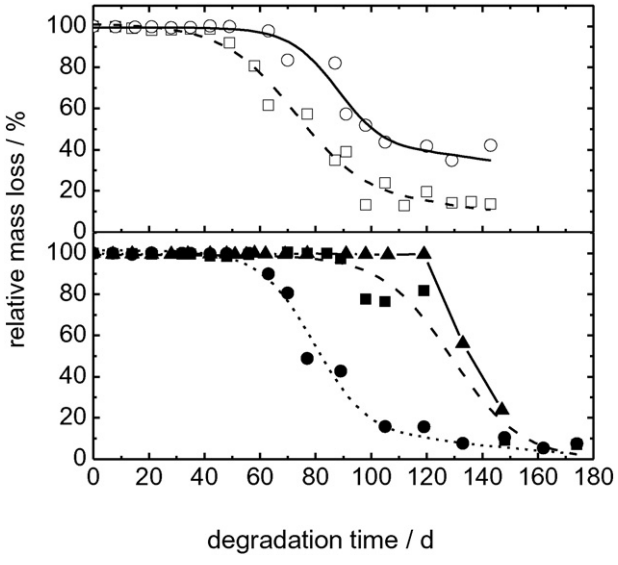

Fig. 19. Hydrolytic degradation of copolyesterurethane networks in aqueous phosphate buffer solution (pH 7) at 37 °C. Relative mass loss as a function of the degradation time; copolyesterurethane networks from three-arm (blank symbols) and four-arm precursors (filled symbols). M_n of the precursors: 1000 g·mol^{-1} (squares), 5000 g·mol^{-1} (circles), and 10,000 g·mol^{-1} (triangles). Adapted from [135] with permission, © 2005 Wiley-VCH Verlag GmbH & Co. KGaA, Weinheim.

Copolyesterurethane networks from four-armed precursors exhibited an induction period of 60–125 days compared with 45–65 days of the polymer networks from the three-armed precursors. The longer induction period is attributed to a slower diffusion in the beginning due to the higher cross-link density.

The effect of the comonomer content on PLGA-based SMP networks was investigated using four polymer networks, providing a glycolide content ranging from 0 wt% to 52 wt%. The induction period decreased significantly when the comonomer content was increased as the ratio of easily hydrolyzable glycolate ester bonds and the hydrophilicity of networks increased (Fig. 20a). Furthermore, the cleavage of ester bonds in the network led to a decrease in the cross-link density so that the swelling of the polymer network will increase and further accelerate degradation.

On the contrary, the relationship between the chemical composition and degradation behavior in SMP networks from copolymers based on *rac*-lactide and comonomers, such as *p*-dioxanone and ε-CL, with different comonomer contents, were studied [75]. In general, in each copolymer network series, higher comonomer content resulted in faster hydrolytic degradation (Fig. 20b). The relative mass loss of poly[(*rac*-lactide)-*co*-(*p*-dioxanone)] and poly[(*rac*-lactide)-*co*-(ε-caprolactone)]-based SMP networks was significantly affected by their thermal properties. When T_g was <37 °C, copolymer networks were rubber-elastic at body temperature facilitating diffusion of water and degradation products. Hence, the mass loss of poly[(*rac*-lactide)-*co*-(ε-caprolactone)] networks having 12 wt% comonomer started earlier than for the copolymer networks based on poly[(*rac*-lactide)-*co*-(*p*-dioxanone)] precursors with 17 wt% comonomer, although glycolate ester bonds have higher hydrolysis rates than hydroxycaproate ester bonds [136].

Therefore, the degradation rate of the copoly(ether)ester urethanes depended not only on the hydrolysis rate of their ester bonds, but also the material hydrophilicity and molecular mobility, which was significantly different at temperatures above or below T_g. Furthermore, it was found that the change of network composition starts much later

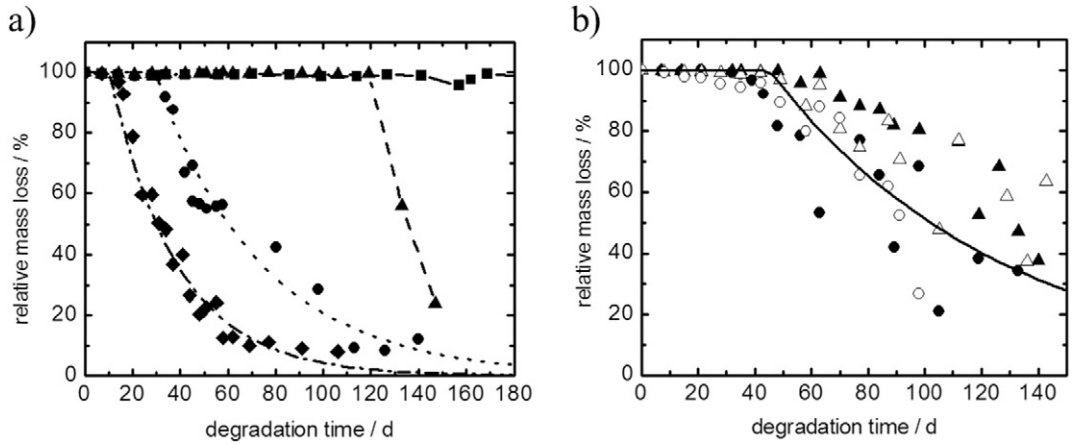

Fig. 20. Relative mass loss as a function of degradation time of copolyesterurethane networks; curves are guidelines for the eye: (a) PLG with glycolide content of 0 wt% (squares), 17 wt% (triangles), 30 wt% (circles), and 52 wt% (diamonds); (b) PLC (filled) and PLD (blank) with comonomer content of 12 wt% (triangles) and 20 wt% (circles). Adapted from [75] with permission. Copyright 2009 American Chemical Society.

than that of architecture, leading to a wave-like changing of T_g. A similar change was observed for ε_b in some networks, which was increased at certain time points, likely due to the formation of entangled nonlinear fragments incorporated into the network. *E* decreased with time in all studied networks, so that an abrupt loss of mechanical properties could be avoided, most notably in the low cross-linked PLG networks [137].

5.2. Enzymatic degradation

In enzymatic degradation, the process of polymer chain scission is catalyzed by the action of enzymes. The enzymes involved in the degradation of biodegradable polymer materials are mainly the nonplasma-specific enzymes, which are, among others, phosphatases, amylases, and lipases. Lipase-type enzymes are responsible for the degradation of polyester-based SMPs [138–141]. The enzymatic hydrolysis process involves several steps such as the diffusion of the enzyme from the surrounding medium to the polymer material, adsorption of the enzyme on the polymer surface, subsequent enzyme–polymer complex formation, and finally after the enzyme action, diffusion of the degradation products from the polymer matrix to the bulk solution.

In case of SMPs with a hydrophobic character, surface erosion by enzymatic degradation is superimposed by a degradation of the inner matrix, as the extracellular enzymes are small enough to penetrate the polymer matrix. The enzymes excreted by microorganisms such as bacteria cleave the ester bond in the polymer structure, reducing the molecular weight and generating small water-soluble fragments. Then, such fragments are transported into the cells to be metabolized by the Kreb cycle, resulting in the formation of carbon dioxide and water (Fig. 18b) [142,143].

It is important to highlight that the enzymatic degradation process is affected by characteristics related to the enzyme used (conformation, concentration, stability, activity) and the chemical and physical properties of the polymeric material (chemical composition, crystallinity, molecular weight, etc.). In addition, chemical modifications of SMPs by grafting functional groups of different natures in the polymeric backbone or copolymerizing monomers (with different characteristics) and varying molar ratios can induce changes in the kinetics and mechanism of enzymatic degradation process.

Recently, the enzymatic degradation of copolymer based on TMC and DLLA, with appropriate monomer feed, were performed using proteinase K at 37 °C. The results have shown a direct dependence between the monomer feed and the enzymatic degradation rates. Poly(1,3 trimethylene carbonate) homopolymers (PTMC) exhibited nonsignificant mass loss within 11 days in contrast to the copolymer materials containing 82% of lactide units, exhibiting 91% of mass loss in the same time period. As a consequence, changes in the morphology and mechanical properties were observed [144].

The enzymatic degradation of block copolymer networks resulting from photocured PLLA-diols and PCL-diols with the photoreactive chain extender 4,4-(adipoyldioxy)-dicinnamic acid with different weight contents was also investigated using *Pseudomonas cepacia* lipase and proteinase K as enzymes [145]. While *P. cepacia* was reported to degrade pure PCL, the proteinase K prefers the cleavage of PLLA bonds. Therefore, the content of PCL and PLLA is an important parameter affecting t_d. A mass loss of about 90% was achieved for a PCL content of 75 wt% within 18 days, whereas the rate of degradation decreased drastically with an increase in the PLLA content when *P. cepacia* was used. On the contrary, the mass loss increased with proteinase K with increasing lactide content, as this enzyme shows a higher substrate specificity for the hydrolysis of PLLA.

6. Summary and conclusion

In this study, SMPs were presented, whereby lactide units contributed in a variety to the network architecture resulting in different functions. PLA chain segments served as permanent netpoints using crystalline domains as well as temporary netpoints using T_g, which was in biomedical application-relevant area. Furthermore, dual-, triple-, and temperature-shape effects were realized, whereby the stimulus could be extended from heat to a water-, light-, magnetic-, and ultrasound-induced SME. The combination with other comonomers or polymers enabled the adjustment of T_{sw}, mechanical, and shape-memory properties.

The additional function of biodegradability generated multifunctional materials, which broadened the fields of application of this interesting material class. While basic research in SMPs is progressing rapidly, in the future, more attention may also be paid to the translation of the materials into clinical applications. Here, first examples of degradable lactide-based SMPs could be shown as drug delivery systems or for the field of tissue engineering. By combining the SME with biodegradability and controlled drug release in one polymeric system, multifunctional materials could be obtained, which open up biomedical applications beyond medical devices. It can be anticipated that the recent advances achieved in shape-memory technology such as reversible bidirectional actuation will be transferred to degradable SMPs based on lactide acid as well. In this way, even the control of the release profiles by the shape-memory actuation can be considered.

Acknowledgments

The authors thank Jorge Luis Escobar Ivirico for preparation of graphics and the Helmholtz Association for programme-oriented funding and funding through the Helmholtz-Portfolio topic "Technology and Medicine."

References

[1] J.H. Henderson, K.A. Davis, R.M. Baker, P. Dubruel, S.V. Vlierberghe, 5—Applications of Shape Memory Polymers (SMPs) in Mechanobiology and Bone Repair, Biomaterials for Bone Regeneration, Woodhead Publishing 2014, p. 111.
[2] K.J. Cha, E. Lih, J. Choi, Y.K. Joung, D.J. Ahn, D.K. Han, Macromol. Biosci. 14 (2014) 667.
[3] A.M. Sammel, D. Chen, N. Jepson, Heart Lung Circ. 22 (2013) 495.
[4] D. Ratna, J. Karger-Kocsis, J. Mater. Sci. 43 (2008) 254.
[5] L.G. Gómez-Mascaraque, R. Palao-Suay, B. Vázquez, M.R. Aguilar, J.S. Román, 12—The Use of Smart Polymers in Medical Devices for Minimally Invasive Surgery, Diagnosis and Other Applications, Smart Polymers and Their Applications, Woodhead Publishing 2014, p. 359.
[6] A. Lendlein, K. Kratz, S. Kelch, Med. Device Technol. 16 (2005) 12.
[7] M. Behl, A. Lendlein, Soft Matter 3 (2007) 58.
[8] A. Lendlein, M. Behl, J. Zotzmann, A. Lendlein, Shape-Memory Polymers and Shape-Changing Polymers, Shape-Memory Polymers, Springer, Berlin Heidelberg 2010, p. 1.
[9] M. Behl, M.Y. Razzaq, A. Lendlein, Adv. Mater. 22 (2010) 3388.
[10] T. Pretsch, Polymer 2 (2010) 120.
[11] P.T. Mather, X.F. Luo, I.A. Rousseau, Annu. Rev. Mater. Res. 39 (2009) 445.
[12] H. Meng, G. Li, Polymer 54 (2013) 2199.
[13] J. Hu, Y. Zhu, H. Huang, J. Lu, Prog. Polym. Sci. 37 (2012) 1720.
[14] C. Liu, H. Qin, P.T. Mather, J. Mater. Chem. 17 (2007) 1543.
[15] Y. Kai, L. Yanjiu, L. Jinsong, Conductive Shape Memory Polymer Composite Incorporated with Hybrid Fillers: Electrical, Mechanical, and Shape Memory Properties, 2011 22/369.
[16] H. Deng, L. Lin, M. Ji, S. Zhang, M. Yang, Q. Fu, Prog. Polym. Sci. 39 (2014) 627.
[17] K.K. Julich-Gruner, C. Löwenberg, A.T. Neffe, M. Behl, A. Lendlein, Macromol. Chem. Phys. 214 (2013) 527.
[18] A. Lendlein, H. Jiang, O. Junger, R. Langer, Nature 434 (2005) 879.
[19] M. Musial-Kulik, J. Kasperczyk, A. Smola, P. Dobrzynski, Int. J. Pharm. 465 (2014) 291.
[20] M. Bao, X. Lou, Q. Zhou, W. Dong, H. Yuan, Y. Zhang, ACS Appl. Mater. Interfaces 6 (2014) 2611.
[21] P. Singhal, W. Small, E. Cosgriff-Hernandez, D.J. Maitland, T.S. Wilson, Acta Biomater. 10 (2014) 67.
[22] A. Ölander, J. Am. Chem. Soc. 54 (1932) 3819.
[23] L. B. Vernon, H. M. Vernon, "Process of manufacturing articles of thermoplastic synthetic resins", US Patent 2234993, 1941.
[24] J. Mohd Jani, M. Leary, A. Subic, M.A. Gibson, Mater. Des. 56 (2014) 1078.
[25] M. Kheirikhah, S. Rabiee, M. Edalat, A Review of Shape Memory Alloy Actuators in Robotics, in: J. Ruiz-del-Solar, E. Chown, P. Plöger (Eds.), RoboCup 2010: Robot Soccer World Cup XIV, Springer, Berlin Heidelberg 2011, p. 206.
[26] D. Stoeckel, Mater. Des. 11 (1990) 302.
[27] F. Butera, Adv. Mater. Process. 166 (2008) 37.
[28] R. Featherstone, Y. Teh, Improving the Speed of Shape Memory Alloy Actuators by Faster Electrical Heating, in: M. Ang Jr., O. Khatib (Eds.), Experimental Robotics IX, Springer, Berlin Heidelberg 2006, p. 67.
[29] F.T. Calkins, J.H. Mabe, J. Mech. Des. 132 (2010) 111012.
[30] S. Echigo, T. Matsuda, T. Kamiya, E. Tsuda, K. Suda, K. Kuroe, Y. Ono, K. Yazawa, ASAIO Trans. 36 (1990) M195.
[31] B. Dietsch, T. Tong, J. Adv. Mater. 39 (2007) 3.
[32] A. Lendlein, R. Langer, Science 296 (2002) 1673.
[33] H.M. Wache, D.J. Tartakowska, A. Hentrich, M.H. Wagner, J. Mater. Sci. Mater. Med. 14 (2003) 109.
[34] S.S. Venkatraman, L.P. Tan, J.F.D. Joso, Y.C.F. Boey, X. Wang, Biomaterials 27 (2006) 1573.
[35] S. Venkatraman, T.L. Poh, T. Vinalia, K.H. Mak, F. Boey, Biomaterials 24 (2003) 2105.
[36] A. Muschenborn, J. Ortega, J. Szafron, D. Szafron, D. Maitland, Biomed. Eng. Online 12 (2013) 103.
[37] J.M. Ortega, J. Hartman, J.N. Rodriguez, D.J. Maitland, Ann. Biomed. Eng. 41 (2013) 725.
[38] A. Lendlein, M. Behl, B. Hiebl, C. Wischke, Expert Rev. Med. Devices 7 (2010) 357.
[39] P. Rychter, E. Pamula, A. Orchel, U. Posadowska, M. Krok-Borkowicz, A. Kaps, N. Smigiel-Gac, A. Smola, J. Kasperczyk, W. Prochwicz, P. Dobrzynski, J. Biomed. Mater. Res. A 103 (2015) 3503.
[40] C. Wischke, A.T. Neffe, S. Steuer, A. Lendlein, J. Control. Release 138 (2009) 243.
[41] C. Wischke, M. Schossig, A. Lendlein, Small 10 (2014) 83.
[42] F. Friess, U. Nochel, A. Lendlein, C. Wischke, Adv. Healthcare Mater. 3 (2014) 1986.
[43] J. Jaworska, K. Jelonek, M. Sobota, J. Kasperczyk, P. Dobrzynski, M. Musial-Kulik, A. Smola-Dmochowska, H. Janeczek, B. Jarzabek, J. Appl. Polym. Sci. (2015) 132.
[44] C. Wischke, A.T. Neffe, S. Steuer, A. Lendlein, Eur. J. Pharm. Sci. 41 (2010) 136.
[45] C. Wischke, A.T. Neffe, S. Steuer, A. Lendlein, Act. Polym. 1190 (2009) 131.
[46] C. Wischke, S. Steuer, A. Lendlein, Mater. Res. Soc. Symp. Proc. 1403 (2012) 207.
[47] C.-Q. Chen, D.-M. Ke, T.-T. Zheng, G.-J. He, X.-W. Cao, X. Liao, Ind. Eng. Chem. Res. 55 (2016) 597.
[48] H. Mitomo, A. Kaneda, T.M. Quynh, N. Nagasawa, F. Yoshii, Polymer 46 (2005) 4695.
[49] C. Wischke, A.T. Neffe, S. Steuer, E. Engelhardt, A. Lendlein, Macromol. Biosci. 10 (2010) 1063.
[50] C. Wischke, S.P. Schwendeman, Int. J. Pharm. 364 (2008) 298.
[51] S.F. Zhang, Y.K. Feng, L. Zhang, J.T. Guo, Y.S. Xu, J. Appl. Polym. Sci. 116 (2010) 861.
[52] Y.K. Feng, S.F. Zhang, H.Y. Wang, H.Y. Zhao, J. Lu, J.T. Guo, M. Behl, A. Lendlein, J. Control. Release 152 (2011) E21.
[53] G. Li, G.X. Fei, H.S. Xia, J.J. Han, Y. Zhao, J. Mater. Chem. 22 (2012) 7692.
[54] M. Bao, Q.H. Zhou, W. Dong, X.X. Lou, Y.Z. Zhang, Biomacromolecules 14 (2013) 1971.
[55] H.M. Chen, Y. Li, Y. Liu, T. Gong, L. Wang, S.B. Zhou, Polym. Chem. UK 5 (2014) 5168.
[56] R. Fernandes, D.H. Gracias, Adv. Drug Deliv. Rev. 64 (2012) 1579.
[57] A. Lendlein, S. Kelch, Angew. Chem. Int. Ed. 41 (2002) 2034.
[58] M. Behl, A. Lendlein, Shape-Memory Polymers, Kirk–Othmer Encyclopedia of Chemical Technology, John Wiley & Sons, Inc. 2011, p. 1.
[59] Q. Shou, K. Uto, M. Iwanaga, M. Ebara, T. Aoyagi, Polym. J. 46 (2014) 492.
[60] R. Kainuma, Y. Imano, W. Ito, Y. Sutou, H. Morito, S. Okamoto, O. Kitakami, K. Oikawa, A. Fujita, T. Kanomata, K. Ishida, Nature 439 (2006) 957.
[61] G. Li, Q. Yan, H. Xia, Y. Zhao, ACS Appl. Mater. Interfaces 7 (2015) 12067.
[62] X.-J. Han, Z.-Q. Dong, M.-M. Fan, Y. Liu, J.-H. li, Y.-F. Wang, Q.-J. Yuan, B.-J. Li, S. Zhang, Macromol. Rapid Commun. 33 (2012) 1055.
[63] A. Yasin, H. Li, Z. Lu, S.u. Rehman, M. Siddiq, H. Yang, Soft Matter 10 (2014) 972.
[64] X. Luo, P.T. Mather, Adv. Funct. Mater. 20 (2010) 2649.
[65] T. Xie, Nature 464 (2010) 267.
[66] K. Kratz, U. Voigt, A. Lendlein, Adv. Funct. Mater. 22 (2012) 3057.
[67] U. Nochel, C.S. Reddy, K. Wang, J. Cui, I. Zizak, M. Behl, K. Kratz, A. Lendlein, J. Mater. Chem. A 3 (2015) 8284.
[68] S. Pandini, S. Passera, M. Messori, K. Paderni, M. Toselli, A. Gianoncelli, E. Bontempi, T. Riccò, Polymer 53 (2012) 1915.
[69] M.Y. Razzaq, M. Behl, K. Kratz, A. Lendlein, Adv. Mater. 25 (2013) 5730.
[70] T. Chung, A. Romo-Uribe, P.T. Mather, Macromolecules 41 (2008) 184.
[71] M. Behl, K. Kratz, J. Zotzmann, U. Nöchel, A. Lendlein, Adv. Mater. 25 (2013) 4466.
[72] M. Behl, K. Kratz, U. Noechel, T. Sauter, A. Lendlein, Proc. Natl. Acad. Sci. 110 (2013) 12555.
[73] M. Saatchi, M. Behl, U. Nochel, A. Lendlein, Macromol. Rapid Commun. 36 (2015) 880.
[74] W. Wagermaier, K. Kratz, M. Heuchel, A. Lendlein, Characterization Methods for Shape-Memory Polymers, in: A. Lendlein (Ed.), Shape-Memory Polymers, Springer, Berlin Heidelberg 2010, p. 97.
[75] A. Lendlein, J. Zotzmann, Y. Feng, A. Alteheld, S. Kelch, Biomacromolecules 10 (2009) 975.
[76] I. Bellin, S. Kelch, R. Langer, A. Lendlein, Proc. Natl. Acad. Sci. 103 (2006) 18043.
[77] B.F. Pierce, K. Bellin, M. Behl, A. Lendlein, Int. J. Artif. Organs 34 (2011) 172.
[78] B. Gupta, N. Revagade, J. Hilborn, Prog. Polym. Sci. 32 (2007) 455.
[79] X. Lu, W. Cai, L. Zhao, Mater. Sci. Forum 475-479 (2005) 2399.
[80] Y.S. Wong, S.S. Venkatraman, Acta Mater. 58 (2010) 49.
[81] M. Radjabian, M.H. Kish, N. Mohammadi, J. Polym. Res. 19 (2012) 1.
[82] K. Paakinaho, H. Heino, M. Pelto, M. Hannula, P. Toermaelae, M. Kellomaeki, J. Mater. Sci. Mater. Med. 23 (2012) 613.
[83] K. Paakinaho, T.I. Hukka, T. Kastinen, M. Kellomaeki, J. Appl. Polym. Sci. 130 (2013) 4209.
[84] Y. Li, S. Xin, Y. Bian, Q. Dong, C. Han, K. Xu, L. Dong, RSC Adv. 5 (2015) 24352.
[85] Y. Ikada, K. Jamshidi, H. Tsuji, S.H. Hyon, Macromolecules 20 (1987) 904.
[86] H. Tsuji, Y. Ikada, Polymer 40 (1999) 6699.
[87] S.R. Andersson, M. Hakkarainen, S. Inkinen, A. Södergård, A.-C. Albertsson, Biomacromolecules 11 (2010) 1067.
[88] T. Kokubo, H.-M. Kim, M. Kawashita, Biomaterials 24 (2003) 2161.
[89] L.L. Hench, J. Am. Ceram. Soc. 81 (1998) 1705.
[90] M. Jarcho, Clin. Orthop. Relat. Res. (1981) 259.
[91] X. Zheng, S. Zhou, X. Li, J. Weng, Biomaterials 27 (2006) 4288.
[92] S. Zhou, X. Zheng, X. Yu, J. Wang, J. Weng, X. Li, B. Feng, M. Yin, Chem. Mater. 19 (2007) 247.
[93] K. Du, Z. Gan, J. Mater. Chem. B 2 (2014) 3340.
[94] X. Zheng, S. Zhou, X. Yu, X. Li, B. Feng, S. Qu, J. Weng, J. Biomed. Mater. Res., Part B 86B (2008) 170.
[95] X. Zheng, S. Zhou, Y. Xiao, X. Yu, X. Li, P. Wu, Colloids Surf., B 71 (2009) 67.
[96] C. Samuel, S. Barrau, J.-M. Lefebvre, J.-M. Raquez, P. Dubois, Macromolecules (Washington, DC, U.S.) 47 (2014) 6791.
[97] C. Samuel, J.-M. Raquez, P. Dubois, AIP Conf. Proc. 1664 (2015) 030005/1.
[98] M. Yamashiro, K. Inoue, M. Iji, Kogyo Zairyo 54 (2006) 30.
[99] M. Yamashiro, K. Inoue, M. Iji, Polym. J. (Tokyo, Jpn.) 40 (2008) 657.
[100] K. Inoue, M. Yamashiro, M. Iji, PMSE Prepr. 93 (2005) 967.
[101] K. Inoue, M. Yamashiro, M. Iji, J. Appl. Polym. Sci. 112 (2009) 876.
[102] M. Xie, L. Wang, J. Ge, B. Guo, P.X. Ma, ACS Appl. Mater. Interfaces 7 (2015) 6772.
[103] A. Petchsuk, W. Klinsukhon, D. Sirikittikul, C. Prahsarn, Polym. Adv. Technol. 23 (2012) 1166.
[104] Y. Huang, P. Pan, G. Shan, Y. Bao, RSC Adv. 4 (2014) 47965.
[105] R. Chang, G. Shan, Y. Bao, P. Pan, Macromolecules (Washington, DC, U. S.) 48 (2015) 7872.
[106] D. Cohn, G. Lando, Biomaterials 25 (2004) 5875.
[107] X.L. Lu, W. Cai, Z.Y. Gao, L.C. Zhao, Mater. Sci. Eng. A A438-A440 (2006) 857.
[108] X.L. Lu, W. Cai, Z. Gao, W.J. Tang, Polym. Bull. (Heidelberg, Ger.) 58 (2007) 381.
[109] X.L. Lu, Z.J. Sun, W. Cai, Z.Y. Gao, J. Mater. Sci. Mater. Med. 19 (2008) 395.
[110] X. Lu, Z. Sun, W. Cai, Phys. Scr., T T129 (2007) 231.

[111] X.L. Lu, W. Cai, Z.Y. Ga, J. Appl. Polym. Sci. 108 (2008) 1109.
[112] L. Peponi, I. Navarro-Baena, A. Sonseca, E. Gimenez, A. Marcos-Fernandez, J.M. Kenny, Eur. Polym. J. 49 (2013) 893.
[113] F. Quaglia, Int. J. Pharm. 364 (2008) 281.
[114] T. Jiang, W.I. Abdel-Fattah, C.T. Laurencin, Biomaterials 27 (2006) 4894.
[115] C. Min, W. Cui, J. Bei, S. Wang, Polym. Adv. Technol. 16 (2005) 608.
[116] J. Wang, J. Li, N. Li, X. Guo, L. He, X. Cao, W. Zhang, R. He, Z. Qian, Y. Cao, Y. Chen, Chem. Mater. 27 (2015) 2439.
[117] I. Navarro-Baena, J.M. Kenny, L. Peponi, Cellulose (Dordrecht, Neth.) 21 (2014) 4231.
[118] I. Navarro-Baena, M.P. Arrieta, A. Sonseca, L. Torre, D. Lopez, E. Gimenez, J.M. Kenny, L. Peponi, Polym. Degrad. Stab. 121 (2015) 171.
[119] L.S. Wang, H.C. Chen, L.F. Zhang, D.L. Chen, X.B. Pang, C.D. Xiong, J. Polym. Res. 18 (2011) 329.
[120] M. Amirian, A.N. Chakoli, J.H. Sui, W. Cai, J. Polym. Res. (2012) 19.
[121] M. Nagata, Y. Yamamoto, Macromol. Chem. Phys. 211 (2010) 1826.
[122] Y.K. Feng, H.Y. Zhao, L.C. Jiao, J. Lu, H.Y. Wang, J.T. Guo, Polym. Adv. Technol. 23 (2012) 382.
[123] T. Shen, M. Lu, D. Zhou, L. Liang, Iran. Polym. J. 21 (2012) 317.
[124] S. Sharifi, D.W. Grijpma, Macromol. Biosci. 12 (2012) 1423.
[125] S. Sharifi, T.G. van Kooten, H.J.C. Kranenburg, B.P. Meij, M. Behl, A. Lendlein, D.W. Grijpma, Biomaterials 34 (2013) 8105.
[126] L.B. Wu, C.L. Jin, X.Y. Sun, Biomacromolecules 12 (2011) 235.
[127] M. Bertmer, A. Buda, I. Blomenkamp-Hofges, S. Kelch, A. Lendlein, Macromolecules 38 (2005) 3793.
[128] N.Y. Choi, A. Lendlein, Soft Matter 3 (2007) 901.
[129] S. Kelch, N.Y. Choi, Z.G. Wang, A. Lendlein, Adv. Eng. Mater. 10 (2008) 494.
[130] A. Lendlein, C. Wischke, K. Kratz, M. Heuchel, J. Zotzmann, B. Hiebl, A.T. Neffe, M. Behl, 1.126—Shape-Memory Polymers, in: P. Ducheyne (Ed.), Comprehensive Biomaterials, Elsevier, Oxford 2011, p. 479.
[131] A. Lendlein, P. Neuenschwander, U.W. Suter, Macromol. Chem. Phys. 199 (1998) 2785.
[132] I. Grizzi, H. Garreau, S. Li, M. Vert, Biomaterials 16 (1995) 305.
[133] E.W. Fischer, H.J. Sterzel, G. Wegner, Kolloid Z. Z. Polym. 251 (1973) 980.
[134] M. Vert, J. Mauduit, S. Li, Biomaterials 15 (1994) 1209.
[135] A. Alteheld, Y. Feng, S. Kelch, A. Lendlein, Angew. Chem. Int. Ed. 44 (2005) 1188.
[136] A. Lendlein, M. Colussi, P. Neuenschwander, U.W. Suter, Macromol. Chem. Phys. 202 (2001) 2702.
[137] A.T. Neffe, G. Tronci, A. Alteheld, A. Lendlein, Macromol. Chem. Phys. 211 (2010) 182.
[138] J. Reiche, A. Kulkarni, K. Kratz, A. Lendlein, Thin Solid Films 516 (2008) 8821.
[139] J.-G. Ryu, Y.-I. Jeong, I.-S. Kim, J.-H. Lee, J.-W. Nah, S.-H. Kim, Int. J. Pharm. 200 (2000) 231.
[140] J.W. Lee, F.-j. Hua, D.S. Lee, J. Control. Release 73 (2001) 315.
[141] M.R. Aberturas, J. Molpeceres, M. Guzmán, F. García, J. Microencapsul. 19 (2002) 61.
[142] H.S. Azevedo, R.L. Reis, Understanding the Enzymatic Degradation of Biodegradable Polymers and Strategies to Control their Degradation Rate, Biodegradable Systems in Tissue Engineering and Regenerative Medicine 2005, p. 177.
[143] D.N. Bikiaris, Polym. Degrad. Stab. 98 (2013) 1908.
[144] J. Yang, F. Liu, L. Yang, S. Li, Eur. Polym. J. 46 (2010) 783.
[145] M. Nagata, Y. Sato, J. Polym. Sci. A Polym. Chem. 43 (2005) 2426.